DETERMINATION OF HONEY CRYSTALLIZATION AND ADULTERATION BY USING TIME DOMAIN NMR RELAXOMETRY

A THESIS SUBMITTED TO
THE GRADUATE SCHOOL OF NATURAL AND APPLIED SCIENCES
OF
MIDDLE EAST TECHNICAL UNIVERSITY

BY

BERKAY BERK

IN PARTIAL FULFILLMENT OF THE REQUIREMENTS
FOR
THE DEGREE OF MASTER OF SCIENCE
IN
FOOD ENGINEERING

AUGUST 2020

Approval of the thesis:

DETERMINATION OF HONEY CRYSTALLIZATION AND ADULTERATION BY USING TIME DOMAIN NMR RELAXOMETRY

submitted by **BERKAY BERK** in partial fulfillment of the requirements for the degree of **Master of Science** i**n Food Engineering, Middle East Technical University** by,

Prof. Dr. Halil Kalıpçılar
Dean, Graduate School of **Natural and Applied Sciences** _____

Prof. Dr. Serpil Şahin
Head of the Department, **Food Engineering** _____

Assoc. Prof. Dr. Mecit Halil Öztop
Supervisor, **Food Engineering, METU** _____

Assist. Prof. Dr. Bekir Gökçen Mazı
Co-Supervisor, **Food Engineering, Ordu University** _____

Examining Committee Members:

Prof. Dr. Serpil Şahin
Food Engineering, METU _____

Assoc. Prof. Dr. Mecit Halil Öztop
Food Engineering, METU _____

Assist Prof. Dr. Bekir Gökçen Mazı
Food Engineering, Ordu University _____

Prof. Dr. Behiç Mert
Food Engineering, METU _____

Assoc. Prof. Dr. Deniz Çekmecelioğlu
Food Engineering, METU _____

Date: 25.08.2020

I hereby declare that all information in this document has been obtained and presented in accordance with academic rules and ethical conduct. I also declare that, as required by these rules and conduct, I have fully cited and referenced all material and results that are not original to this work.

Name, Last name: Berkay Berk
Signature:

ABSTRACT

DETERMINATION OF HONEY CRYSTALLIZATION AND ADULTERATION BY USING TIME DOMAIN NMR RELAXOMETRY

Berk, Berkay
Master of Science, Food Engineering
Supervisor: Assoc. Prof. Dr. Mecit Halil Öztop
Co-Supervisor: Assist. Prof. Dr. Bekir Gökçen Mazı

August 2020, 97 pages

Honey is an important source of sugar and widely used as a natural sweetener. The demand for honey has increased significantly due to increase in the consumer tendency to use natural sugars as an alternative to starch based sweeteners (SBS). Thus, honey as being expensive compared to SBS has become very susceptible to adulteration and started to suffer from significant quality problems.

In addition to adulteration, crystallization is another problem that could affect the quality of the honey. Crystallization is a natural process that could occur in honey due to several reasons and precipitation of glucose is one of them. In this study, a non-conventional TD-NMR pulse sequence: *Magic Sandwich Echo (MSE)* was used to monitor the crystallization of honey at 14°C. Honey samples were seeded with glucose to induce crystallization and samples were monitored for 96 hours. T_1 and T_2 relaxation times were measured during the process to follow changes in the state of water. Mono-exponential and bi-exponential relations were used to explain T_1 and T_2 relaxation times, respectively. As a complementary method to NMR, crystal melting enthalpy was also measured by differential scanning calorimetry (DSC). High correlations were detected between NMR and DSC results (r=0.87). During crystallization, T_1 relaxation times did not change, whereas both components of T_2 decreased with increasing time.

Besides crystallization, MSE sequence was used to detect adulteration of honey by glucose (GS) and high fructose corn syrups (HFCS) accompanied with T_1 and T_2 relaxation time measurements. Mono-exponential and bi-exponential relations were also used to explain T_1 and T_2, respectively in this part of the study. Higher maltose in GS (r=0.96) and changing glucose to water ratio of HFCS (r=0.91) gave high correlations with the MSE output. In both HFCS and GS adulteration, two different proton pools of T_2 were detected. Addition of GS resulted in decrease in fast-relaxing component of T_2 time due to decreased mobility. All components of T_2 time increased with HFCS addition due to higher water content of HFCS resulting in higher mobility.

In addition to crystallization and adulteration, the melting of crystallized honey was also performed at 50℃ inside the NMR system. Crystal melting was monitored in real-time, and the rate of crystal removal was fitted to a mono-exponential decay model.

Results obtained from NMR experiments showed that TD-NMR is a powerful technique to investigate crystallization, detect adulteration and monitor melting of honey samples.

Keywords: Honey, crystallization, adulteration, TD-NMR, MSE

ÖZ

ZAMANSAL ALANDA NMR RELAKSOMETRE KULLANARAK BALDA KRİSTALLENME VE TAĞŞİŞİN BELİRLENMESİ

Berk, Berkay
Yüksek Lisans, Gıda Mühendisliği
Tez Yöneticisi: Doç. Dr. Mecit Halil Öztop
Ortak Tez Yöneticisi: Dr. Öğr. Üyesi Bekir Gökçen Mazı

Ağustos 2020, 97 sayfa

Bal önemli bir şeker kaynağıdır ve doğal bir tatlandırıcı olarak yaygın şekilde kullanılmaktadır. Tüketicinin nişasta bazlı şekerlere alternatif olarak balı kullanma eğilimindeki artış dolayısıyla bal arzı önemli ölçüde artmıştır. Böylelikle, şeker şuruplarına kıyasla pahalı olduğu için bal, tağşişe karşı çok duyarlı hâle gelmiştir ve önemli kalite sorunlarıyla karşı karşıyadır.

Tağşişe ek olarak, kristalleşme balın kalitesini etkileyebilecek başka bir sorundur. Kristalleşme, çeşitli sebepler yüzünden balda doğal olarak meydana gelen bir durumdur ve glikozun çökelmesi bu sebeplerden biridir. Bu çalışmada, 14°C'deki kristalleşmeyi takip etmek için geleneksel olmayan bir TD-NMR puls sekansı olan *Sihirli Sandviç Eko (MSE)* kullanılmıştır. Kristalizasyonu tetiklemek için bal örnekleri glikoz ile tohumlanmıştır. T_1 ve T_2 relakasyon zamanları da süreç boyunca ölçülmüştür. Sırasıyla, T_1 ve T_2 zamanlarını açıklamak için tek üstel ve çift üstel ilişkiler çalışmanın bu kısmında da kullanılmıştır. NMR'a tamamlayıcı bir yöntem olarak, kristal erime entalpisi diferansiyel taramalı kalorimetri (DSC) yöntemi ile ölçülmüştür. NMR ve DSC sonuçları arasında yüksek bağıntılar tespit edilmiştir (R=0.87). Kristalizasyon süresince, T_1 zamanında değişim gözlenmezken T_2 zamanının her iki bileşeni de zamanla azalmıştır.

Kristalizasyonun yanında, MSE dizini, T_1 ve T_2 relaksasyon zamanları ile birlikte balın glikoz şurubu (GS) ve yüksek fruktozlu mısır şurubu (HFCS) ile tağşişinin tespitinde kullanılmıştır. Sırasıyla, T_1 ve T_2 zamanlarını açıklamak için tek üstel ve çift üstel ilişkiler kullanılmıştır. Glikoz şurubunun yüksek maltoz içeriği (R=0.96) ve yüksek fruktozlu mısır şurubunun değişen glikoz/su oranı (R=0.91) MSE çıktısı ile yüksek bağıntı vermiştir. Hem HFCS hem de GS tağşişlerinde, T_2 zamanının 2 farklı proton havuzu tespit edilmiştir. GS eklenmesi, azalan hareketlilik yüzünden T_2 zamanının hızlı relakse olan bileşeninde azalma ile sonuçlanmıştır. T_2 zamanının tüm bileşenleri, HFCS'in yüksek su içeriği yüzünden artan hareketlilik sonucu artan HFCS miktarıyla birlikte artmıştır.

Kristalizasyon ve tağşişe ek olarak, kristallenmiş balın erimesi de NMR sisteminin içinde 50℃'de gerçekleştirilmiştir. Kristal erimesi gerçek zamanlı olarak takip edilmiş ve kristal erime hızı tek üstel bozunma eğrisi ile modellenmiştir.

NMR deneylerinden elde edilen sonuçlar, TD-NMR'ın bal örneklerinin kristalizasyonunun incelenmesinde, tağşişinin belirlenmesinde ve erimesinin takip edilmesinde güçlü bir teknik olduğunu göstermiştir.

Anahtar Kelimeler: Bal, kristallenme, tağşiş, TD-NMR, MSE

To best of bests, my beloved family…

ACKNOWLEDGMENTS

I would like to express my gratitude to my supervisor Assoc. Prof. Dr. Mecit Halil Öztop for his guidance, advice, criticism, encouragements and insight throughout the research. Also, it is the greatest pleasure of me to be a part of his team as both undergraduate and master student.

I would like to offer my special thanks to my best friends who I met in the beginning of my high school years and filled even half of my life with their unconditional friendship; Yunus Keskin, Oğuz Aydınbelge and Hasan Akalp. Besides them, I also would like to thank my chemistry teacher; Lütfiye Büken. With her guidance, I liked and chose science.

My special gratitude goes to my close friends who have not left me alone for any reason since the beginning of my undergraduate study; Oğuz İren, Yasin Şencan, Emre Çetinaslan, Yusuf Bilen, Elif Över and Aysu Deniz. They have been standing with me for years and during those years, they witnessed to my evolution to choose the academic life. I think, my undergraduate life would not be this much satisfying without them.

I would like to thank my lab friends; Begüm Köysüren, Eda Ceren Kaya, Ülkü Ertuğrul, Şirvan Sultan Uğuz, Ozan Taş and Muhammad Bin Zia for their forever joy and providing me funny moments. I do not think that there is another lab team like this on the earth.

My very special gratitude belongs to Bilge Baştürk who covered my all master life and gave continuous support. I could not finish this study without her aid. I can say that one of the best things that ever happened to me is to meet her.

Last but not the least, I express my deepest gratitude to my family. My father İsmail, my mother Sema and my brother Mehmet always encouraged me about academic life. I cannot verbalize their contribution to this study and my entire life.

This work is funded by The Scientific and Technological Research Council of Turkey (TÜBİTAK) with the proposal number 217O089 under 1001 Programe.

TABLE OF CONTENTS

LIST OF TABLES

TABLES

LIST OF FIGURES

FIGURES

LIST OF ABBREVIATIONS

CC : Crystal content
DP3 : Sugar consisting of 3 monosaccharides
DP4 : Sugar consisting of 4 monosaccharides
DPn : Sugar consisting of n monosaccharides
DSC : Differential scanning calorimetry
ERH : Equilibrium relative humidity
FID : Free induction decay
Fru: : Fructose
FTIR : Fourier transform infrared
G/W : Glucose to water ratio
Glu : Glucose
GS : Glucose syrup
HFCS : High fructose corn syrup
HPLC : High performance liquid chromatography
IR : Infrared
IRMS : Isotope ratio mass spectroscopy
IS : Invert syrup
KF : Karl Fischer
LF : Low field
Mal : Maltose
MC : Moisture content
MSE : Magic sandwich echo
NMR : Nuclear magnetic resonance
RF : Radiofrequency
RID : Refractive index detector
SBS : Starch based sugar
SE : Solid echo
SFC : Solid fat content
TD : Time domain

LIST OF SYMBOLS

α_w : Water activity

ρ : Population value

τ_{cr} : Time at which 63.21% of the maximum amount of crystal is formed

τ_{φ} : Phase cycling time

L* : Lightness value form black (0) to white (100)

a* : Color value from green (-) to red (+)

b* : Color value from blue (-) to yellow (+)

CHAPTER 1

INTRODUCTION

1.1 Honey

Honey is a sweet secretion consisting of several sugars and other components and produced by Honeybee species (*Apis* spp.) mainly (Eva Crane, 1991). Almost all honey sold in the markets is produced by the species *Apis mellifera* (see Fig. 1.1) also called Western Honeybee. Honey was an important sweetener in the history, even before than the cane (or beet) sugar had become common. In these days, due to tendency to consume natural products, it is also added to commercial products to provide sweetness naturally (Mesías et al., 2019). In addition to be used as an additive for sweetening purposes, it was also used as the substrate for fermentation. The wine produced by using honey is called "Mead". Mead was produced for centuries in Africa, Europe and Asia (Hornsey, 2003). Also, it had a place in some mythologies like Norse mythology. Moreover, in most of the cultures, honey is an essential part of breakfast (Batt & Liu, 2012; Cosmina et al., 2016; Šedík et al., 2018). Due to this much of tendency for consumption, honey is a valuable food product.

In Turkey, it was reported that 105,727 tons of honey was produced in 2017 and Turkey is in the second order in the countries that are producing honey (Burucu, 2017).

Figure 1.1. Western Honeybee *Apis mellifera*

1.2 Composition of Honey

Honey mostly consists of sugars that are fructose, glucose, maltose, sucrose, and higher saccharides. An example composition is provided in Table 1.1:

Table 1.1 Biochemical composition of honey (McGee, 1984)

Component	Percentage Weight (%)
Water	17
Fructose	38
Glucose	31
Sucrose	2.5
Other Disaccharides	8.0
Higher Sugars	2.5
Acids	0.6
Minerals	0.2
Proteins	0.2

As seen from Table 1.1, major constituents of honey are sugars. Due to its low water content, it is also called a supersaturated mixture. This supersaturation in honey makes it is more prone to glucose precipitation which is also known as ‘honey crystallization’.

1.3 Honey Types

According to Codex Alimentarius, honey is classified into two main group in terms of botanical origin: blossom honey and honeydew honey (Codex Alimentarius Commission, 2001a). In Turkey, both types present. While honeydew honey is mostly collected from the regions that have pine trees, blossom honey is collected from everywhere.

1.3.1 Blossom Honey

As mentioned before, honey is the sweet secretion of honeybees that are fed by sweet parts of plants. When this feed is the nectar from the plants, resulting honey becomes blossom honey. There are various plants to be a source of nectar for honeybees. Most common ones are acacia, buckwheat, chestnut, lavender, orange blossom, and thyme. Due to aromatic compounds of the plant nectar, the resulting honey also has different characteristics inherently. Over 400 different aromatic compounds are detected in honey (Bentivenga et al., 2004). Those aromatic volatile compounds are so strong that even origin of honey can be detected with respect to a group of specific compounds (Moreira et al., 2002).

1.3.2 Honeydew Honey

In addition to nectar of plants, honeybees can also be fed by other sweet compounds. The secretion of some insects living on the trees could be an example. Therefore, it is possible to say that the resulting honeydew honey is a product of cooperation of two different organisms (de-Miguel et al., 2014). Firstly, the insect produces a secretion from the plant, then the honeybee consumes this secretion and produces honey. In Turkey, most of the honeydew honey has origin of the pine trees (*Pinus brutia*) which is called *Turkish Pine* (E Crane, 1999). The most abundant insects on this process are called scale insects, and especially *Marchalina hellenica* species

(Gounari, 2006). It was stated that pine honey has a darker color and spicy aroma when compared to blossom honeys (Marchese, 2009).

1.4 Physical Properties of Honey

1.4.1 Water Activity

Honey is a perfect medium containing tremendous amount of nutrients. These nutrients are not only the interest of human or animals. Besides, microorganisms could utilize the nutrients for fermentation purposes, especially yeasts. As a result of this, honey can be spoiled due to fermentation products of the microorganisms. The major opportunity to develop a yeast on the honey is the relatively high moisture content (Root & Root, 1919). However, direct expression of moisture content is not sufficient to explain the microbial growth factor since the water that can be utilized by microorganisms is free (or available) water. There is a discrimination in the state of water due to interaction with other materials in the matrix. These interactions make the water bounded (Caurie, 2011). There is this concept that explains the chemical potential of water in the systems called water activity (α_w). Water activity is the ratio of vapor pressure of water in the matrix to the vapor pressure of standard state pure water (Brunauer et al., 1938). To express whether a microorganism can survive in a medium or not, α_w value is used. The α_w value gives information about available water in the medium, which is utilized by the microorganisms.

1.4.2 Moisture Content

As in Table 1.1; water content of honey is low when compared to liquid foods. Due to high solubility of sugars in honey and low water content, it makes the state supersaturated. The presence of water in the matrix gives fluidity to the material. By this fluidity, there is movement of the components in the matrix. This phenomenon is called molecular mobility, which is the capacity of the molecules to move. Honey

crystallization is a process induced by the movement of the glucose molecules. To express the tendency of honey to crystallize, glucose to water ratio is used. Since the denominator of the ratio is water, moisture content is an important factor to determine quality of honey in terms of crystallization (Dyce, 1975). Moisture content of honey influences the fluidity and other textural properties like adhesiveness (Yener et al., 1987). The amount of water affects the α_w and hence the probability of microbial growth too. In water content measurements, there are various methods, but most of them relies on weight loss on drying. There are various studies on weight loss depended methods such as hot air dryer (Gill et al., 2015; Yener et al., 1987), hot water dryer (Subramanian et al., 2007), microwave vacuum dryer (Cui et al., 2008). Another practical approach is the measurement of refractive index by correlating with some empirical relationships (International Honey Commission (ICH), 2009). This is a fast, cheap and accessible technique, but the main drawback is lower applicability in non-liquified honey samples. In other words, this method does not work for crystallized honey samples. Furthermore, the empirical equations could not be valid for all types of honeys. To measure low water content in these types of systems, there is a coulometric method which is also known as Karl Fischer titration. The basis of this method relies on electrical potential difference of elemental iodine and ionic iodine that are produced in titration medium because of water presence.

1.4.3 Sugar Composition of Honey

Biochemical composition of honey is shown in Table 1.1. The majority of sugars belongs to monosaccharides, which are glucose and fructose.

Glucose is a six carbon monosaccharide having water solubility of 47 g glucose per 100 g of solution at 20°C (Alves et al., 2007). Haworth projection of glucose is given in Fig. 1.2.

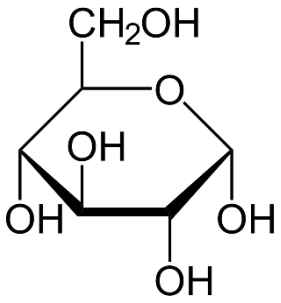

Figure 1.2. Haworth projection of D-Glucose

As seen on the Fig. 1.2; the backbone is hexagonal, which is called pyranose. Abundance of glucose is wide in fruit and vegetables (Carter et al., 2013). In addition to glucose, there is another important monosaccharide in honey: fructose. Fructose is also a 6 carbon monosaccharide having water solubility of 79 g fructose per 100 g of solution at 20°C (Crestani et al., 2013). Haworth projection of fructose is given in Fig. 1.3.

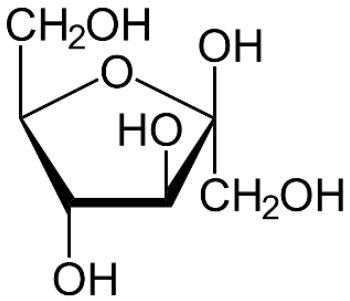

Figure 1.3. Haworth projection of D-Fructose

Different from glucose, fructose is in pentagonal shape despite it has same number of carbons. Also, glucose and fructose are isomers of each other. As happens in the case of glucose, abundance of fructose is also wide in fruit and vegetables (Carter et al., 2013). In daily language, fructose is also called fruit sugar. As indicated in Table 1.1, majority of the sugars in honey are monosaccharides. However, besides monosaccharides, there are also disaccharides and higher sugars that are present in

honey. One of those disaccharides is sucrose. Sucrose is a dimer composed of 1 glucose and 1 fructose molecules and its solubility in water is 67 g sucrose per 100 g of solution at 20°C (Crestani et al., 2018). Sucrose is mostly produced from sugar beet and sugarcane. In fruits, occurrence of sucrose is not high as compared to glucose and fructose. Chemical structure of sucrose is given in Fig. 1.4.

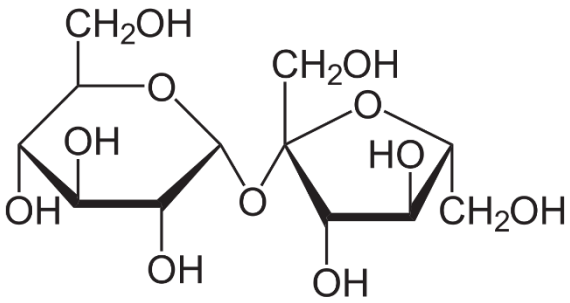

Figure 1.4. Haworth projection of Sucrose

Sucrose is the reference point for sweetness perception. In other words, sweetness values of all other sugar ad sugar like substances are reported as relative sweetness to 1.00, which is the sweetness of sucrose. There is another disaccharide in honey which is maltose. Maltose is a dimer consisting of two glucose molecules and water solubility of maltose is 48 g maltose per 100 g of solution (Gong et al., 2012). Maltose is not used as a sweetener due to its low sweetness. Haworth projection of maltose can be seen in Fig. 1.5.

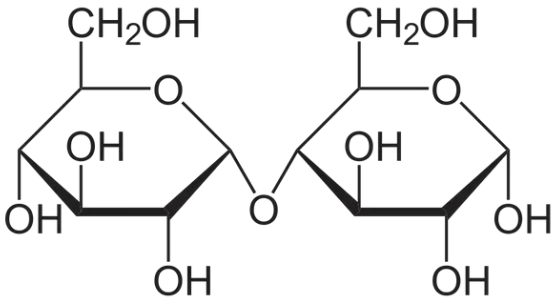

Figure 1.5. Haworth projection of Maltose

Not a major presence in honey, but there is also one polymeric form of glucose which is starch. Starch is composed of two different structured glucose polymers, which are amylose (see Fig. 1.6) and amylopectin (see Fig. 1.7).

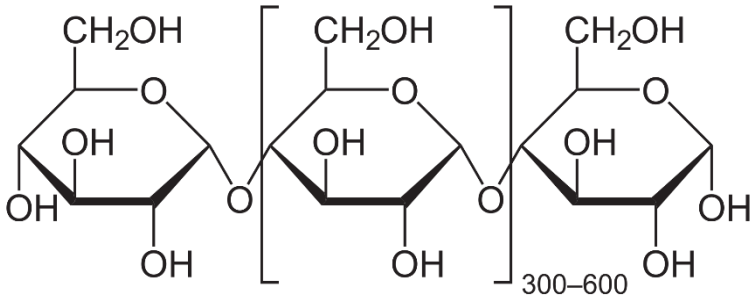

Figure 1.6. Amylose

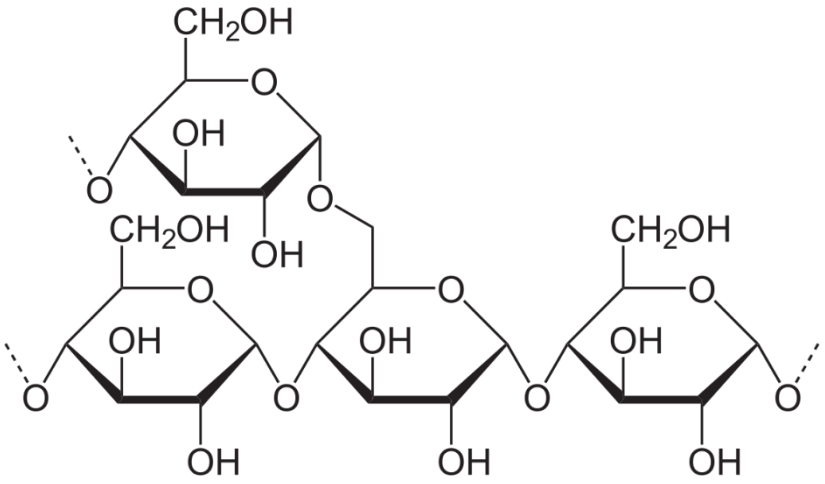

Figure 1.7. Amylopectin

Depending on the source, starch generally contains 20-25% amylose and 75-80% amylopectin (Solomons et al., 2016). This composition significantly affects the physicochemical properties of starch such as gelling, pasting and hardness that are important for determination of honey adulteration (Ma et al., 2017).

1.4.4 Viscosity of Honey

Viscosity is a measure of resistance of a fluid to flow (Şahin et al., 2016). Honey is classified as a viscous fluid due to low water content. There are factors affecting honey viscosity such as temperature, water content and crystallinity. Since botanical origin changes the organoleptic properties of honey, it could be thought that it also affects viscosity. However, it was studied that there is relatively small difference on the viscosity of different botanical originated honey samples having the same water content (Rybak-Chmielewska & Szczesna Pulawy (Poland). Apiculture Division), 1999). Temperature significantly affects viscosity of all materials. As honey is heated, internal frictional forces are depressed and so the honey becomes more fluid. In other words, as temperature increases, viscosity of honey decreases. This relationship can be explained by Arrhenius equation (Gómez-díaz et al., 2009). In the combination of temperature and water content, it was observed that at lower temperatures, water content influences the viscosity significantly but at higher temperatures not (Bakier, 2017). Besides these, as crystallinity of honey is altered, viscosity is affected due to particle formation in the matrix. It was reported that there is a potential to measure the crystal content of honey by measuring the viscosity (Al-Habsi et al., 2013) and potential to determine adulteration by viscosity (Yilmaz et al., 2014).

Table 1.2 Viscosity values of different honey samples

Honey Type	Viscosity (Pa.s)	Reference
Australian	34.40	(Al-Habsi et al., 2013)
Acacia	36.50	
Chinese	8.03	
Brazilian	3.13	
Turkish	6.53	(Yilmaz et al., 2014)
Poland	12.95	(Bakier et al., 2016)
Spain	10.25	(Gómez-díaz et al., 2009)

1.4.5 Color of Honey

Color is the first quality attribute detected by consumers. Therefore, color of honey is an important parameter for its acceptability. It was stated that the pigments presenting in honey mostly belong to phenolic compounds and non-enzymatic browning end products (Belitz et al., 2004). The color of honey can range from water white to dark amber with respect to their botanical origin, content of phenolic substances and non-enzymatic browning reaction results (Boukraâ, 2013). To characterize honey in terms of color, the most common method is measuring the color intensity and coordinates spectrophotometrically and then compare with Pfund Scale (Escuredo et al., 2019). Each botanical source contribute different color characteristics, so it could be possible to differentiate honey authenticity by color by setting up libraries (Tuberoso et al., 2014). To set up a concrete method for measuring color, several characterization studies based on reflectance spectroscopy accompanied by CIEL*a*b system (Escriche et al., 2012, 2017), digital honey colorimetry (Fechner et al., 2020) and sensory color comparison with respect to Pfund grader system(Belay et al., 2015; Serra Bonvehi et al., 2019) were conducted. All methods consisted of measuring color of honey by a system and comparing with the reference Pfund scale. When a powerful database is structured and supported with already driven methods, it could be easy to determine honey type and origin by color measurement.

Table 1.3 Color index values of different honey samples

Botanical Origin	L*	a*	b*	Reference
Asphodel	86.7±4.3	-2.0±0.7	37.2±14.2	
Buckwheat	41.3±2.7	30.9±1.6	71.2±3.8	
Black locust	87.2±1.6	-1.5±0.2	17.6±3.3	
Sweet chestnut	63.0±4.8	18.1±4.3	82.7±8.8	
Citrus	81.1±4.9	-0.8±1.8	29.8±4.6	
Savory	62.1±7.2	16.3±4.5	71.0±6.5	
Garland thorn	76.1±6.5	3.9±2.4	52.3±8.8	(Tuberoso et al., 2014)
Thistle	79.2±3.4	0.8±1.8	58.1±7.1	
Lime	78.4±4.2	1.9±0.7	53.6±12.8	
Mint	44.2±7.5	26.9±4.6	70.0±9.6	
Rapeseed	81.2±3.9	-0.5±0.5	30.9±7.2	
Sage	82.4±5.8	1.6±3.6	56.9±10.2	
Strawberry tree	66.3±5.6	12.5±3.7	71.8±5.3	
Eucalyptus	72.8±6.3	3.8±2.2	52.6±7.5	(Tuberoso et al., 2014)
	75.4±5.4	2.6±4.4	28.7±4.2	(Escuredo et al., 2019)
Heather	66.1±3.8	12.0±2.8	68.6±3.1	(Tuberoso et al., 2014)
	56.1±2.9	10.9±2.1	11.0±2.2	(Escuredo et al., 2019)
Honeydew	47.1±9.6	23.3±7.3	65.8±7.6	(Tuberoso et al., 2014)
	51.6±3.6	8.8±2.8	7.4±2.9	(Escuredo et al., 2019)
Blackberry	73.5±6.1	4.0±5.0	27.5±3.5	(Escuredo et al., 2019)
Chestnut	53.0±2.3	9.9±1.4	11.1±2.2	(Escuredo et al., 2019)

1.4.6 Electrical Conductivity

Measurement of electrical conductivity of honey indicates some characteristic properties like whether it is blossom or honeydew honey and even its botanical source (Vorwohl, 1964). The differentiation comes from the minerals, organic acids, polyols contents and proteins in honey (Eva Crane, 1975). Since the electrical conductivity vary depending on ionizable solute concentration, it was standardized that the reported electrical conductivity is the measured electrical conductivity of 20% (w/v) weighted honey in solution at 20℃ in milli Siemens per centimeter (mS/cm) (Acquarone et al., 2007). Popek (2002) studied a procedure to identify the type of honey and found that electrical conductivity accompanied by acidity measurement was a significant method to estimate the botanical source of honey. Terrab et al. (2003) studied correlation between the mineral type and electrical conductivity in Morocco honey to estimate the effect of different minerals on electrical conductivity.

Table 1.4 Electrical conductivity values of different honey samples

Honey Type	Electrical Conductivity ($S.cm^{-1}\ 10^{-4}$)	Reference
Acacia	2.19±0.49	(Popek, 2002)
Linden	5.49±0.34	
Multifloral	6.84±0.40	
Buckwheat	3.57±0.35	
Heather	6.09±0.15	
Rape	3.56±0.29	
Honeydew	9.97±0.60	
Nectar-honeydew	9.38±1.22	

1.4.7 pH of Honey

As a plant source, there are many organic acids present in honey. Anklam (1998) found 32 different aliphatic dicarboxylic acids by using a gas chromatography – mass spectroscopy (GS-MS). Since these organic acids originated from the plant source of the honey, it gives an idea about the type of honey. Wilkins & Lu (1995) proposed two different organic acids as markers for New Zealand rewarewa honeys. Due to the presence of these organic acids, honey has a pH range of 3.50-5.50 (Sereia et al., 2017). Yadata (2014) studied different honey samples by measuring the electrical conductivity and pH during seasons and concluded that darker honeys had lower pH values than lighter ones due to the presence of phenolic substances in darker honeys. pH of honey could also be a criterion to estimate the sugar syrup addition due to absence of acidic compounds in syrups.

Table 1.5 pH values of different honey samples from Ethiopia

Honey Type	pH	Reference
Gbito	4.17±0.13	(Yadata, 2014)
Mexi	3.96±0.01	
Shako	3.96±0.01	
Korcha	4.00±0.01	

1.5 Quality Problems of Honey

1.5.1 Honey Crystallization

The water content of honey is low, and major components are fructose and glucose. Due to this low water content, honey is prone to crystallization. Crystallization in honey is defined as the precipitation of glucose in the form of glucose monohydrate due to the supersaturated nature of the honey (Zamora & Chirife, 2006). Crystallization is an undesirable process except for the cream honey production. This is because physicochemical properties like viscosity and water activity are affected (Laos et al., 2011). As crystallization proceeds, water activity increases, and honey becomes more susceptible to microbial growth. In addition to the glucose content, there are other intrinsic factors influencing crystallization, such as pre-formed crystal or the presence of impurities. Other than the intrinsic factors, environmental conditions are also important in the crystallization of honey. Since crystallization is directly related to the mobility of glucose present in honey, viscosity is an important parameter on the crystallization. Viscosity is composition dependent intrinsically, but also temperature dependent. As temperature decreases, viscosity increases, and molecular mobility of glucose is lowered. However, with lower temperature, solubility of glucose also becomes less. Therefore, it is not true to say that lower temperatures triggers crystallization directly. There is an optimum range for crystallization (Al-Habsi et al., 2013). There is also fructose present in honey, but it does not contribute to crystallization due to its solubility being higher than glucose.

Besides crystallization itself, the rate of crystallization is also important since it is a dynamic process. How fast crystallization occurs under which conditions provides the ability to monitor and control the process. To determine the crystallization rate, there are various methods that rely on measuring the crystal content present in the honey. Some of these are based on measuring water activity, sugar profile, and melting enthalpy. For the water activity case; as honey is crystallized, glucose

interacts with water and precipitates in the form of glucose monohydrate. Due to lower interaction with water, the water activity of the sample increases (Gleiter et al., 2006). In the sugar profile analysis, the sugar composition of the supernatant part of the centrifuged crystalline honey is examined. Based on the assumption that crystallization occurs due to only glucose content, with a simple mass balance calculation, the crystal amount is calculated (Al-Habsi et al., 2013). For the melting enthalpy approach, the crystallized honey sample is thermally treated, and the energy required to melt the crystal is measured. With the correlation of energy needed and mass, the amount of crystal portion is determined (Lupano, 1997).

1.5.2 Honey Adulteration

Since honey is produced by bees and has a limited production capacity, there are some improper ways to obtain more honey with less cost; and one way is adulteration. Adulteration is defined as the addition of another substance to the nature of food to increase the quantity. In addition to this, there are different ways of adulteration such as physical treatments so as to show the material more qualified. According to Codex Alimentarius, it is prohibited to adulterate honey (Codex Alimentarius Commission, 2001b). Common adulterants added to honey are agave, maple, sugar cane, barley, corn and rice syrups. Due to higher yield and accesibility, corn syrup is the most common one among them.

High fructose corn syrup (HFCS) is a sweetener produced from corn starch. Starch in the corn is firstly extracted and then the obtained starch is enzymatically hydrolyzed (Amaral-Fonseca et al., 2020). The product of this process is a mixture of glucose, maltose and other oligosaccharides of glucose. This mixture is called glucose syrup (GS). Since the sweetness of glucose is not high, it is converted to fructose by isomerization. Most common product of this isomerization process is called HFCS-42 which has 42% of fructose, 50% of glucose and 8% of other sugars in sugar basis (Keim et al., 2015). Due to these fractions, HFCS has similar chemical

composition and sweetness to honey. When those syrups are added to honey, it cannot be easy to understand whether it is adulterated or not by organoleptic analysis. For those cases, analytical methods are needed. For determination of adulteration, there are various methods having mostly the basis of chromatography and spectroscopy.

In the study of Wang et al. (2020), differently from common adulteration, resin adsorption was analyzed by using high performance liquid chromatography (HPLC) with electrochemical detection (ECD) system. It was found that organic acid profile of raw acacia honey could be a variable to distinguish resin adsorption adulteration. Another adulteration detection method is based on stable isotope ratios. The nectar for honey production is collected mostly from C3 plants such as rice and sugar cane. The minority of nectar is collected from the C4 plants such as corn and sugarcane. Therefore, detection of C4 sugar addition is easier than C3 sugar addition due to the major C3 plant nectar in honey.

Besides separation, there are direct spectroscopic methods that can be used for detecting adulteration. Infrared (IR) spectroscopy is one of the most common techniques used for this purpose. Gallardo-Velázquez et al., (2009) studied Fourier transform infrared (FTIR) spectroscopy in mid spectral region (4000–650 cm^{-1}) to detect GS, HFCS and invert syrup (IS) adulteration and concluded that it was a successful technique when accompanied with multivariate analysis. According to Se et al. (2019), it is possible to detect even C3 sugar adulteration by IR spectroscopy. As another spectroscopic technique, isotope ratio mass spectrometry (IRMS) was used to detect adulteration. As mentioned before, majority of the nectar used in honey production has C3 sugars. Therefore, addition of C4 sugars can be detected by altered ^{13}C to ^{12}C ratio in the medium. Çinar et al. (2014) studied pine honey samples adulterated with HFCS by IRMS and stated that this method was a powerful technique to detect C4 sugar adulteration. There is another way to determine carbon isotope ratio in honey; nuclear magnetic resonance (NMR) spectroscopy. Giraudon

et al. (2000) performed high field deuterium nuclear magnetic resonance spectroscopy using a 9.4 T cryomagnet and concluded that deuterium NMR spectroscopy provides C3 sugar detection on honey adulteration. However, the main drawbacks of these instruments are requirement of trained personnel and high maintenance and initial investment costs.

1.6 Advanced Characterization Techniques That Can Be Used for Honey Samples

There are various methods and characteristics of honey as mentioned before. In addition to those common methods there are different ways to investigate the different properties of honey. In this study, differential scanning calorimetry (DSC) and time domain nuclear magnetic resonance (TD-NMR) relaxometry have been used as the two advanced characterization techniques. A slight background of these techniques is provided in this section.

1.6.1 Differential Scanning Calorimetry (DSC)

Differential scanning calorimetry is a thermo-analytical tool to measure the heat response of a material as a result of applied temperature change (Chiu & Prenner, 2011). It is mostly used for determination of phase change and thermodynamic properties of materials (Jelesarov & Bosshard, 1999). A DSC instrument contains two chambers: one for sample and one for the reference material. Both chambers are initially at the same temperature and then they are heated or cooled with respect to a defined temperature program and the temperature difference of the reference material and sample is measured. In terms of thermal chamber configurations, there are two types of DSC; power compensated and heat flux DSC. As indicated by the names, power compensated DSC keeps the power supply constant whereas heat flux DSC keeps the heat flux constant. Schematic representation of a heat flux DSC cell is shown in Fig. 1.8.

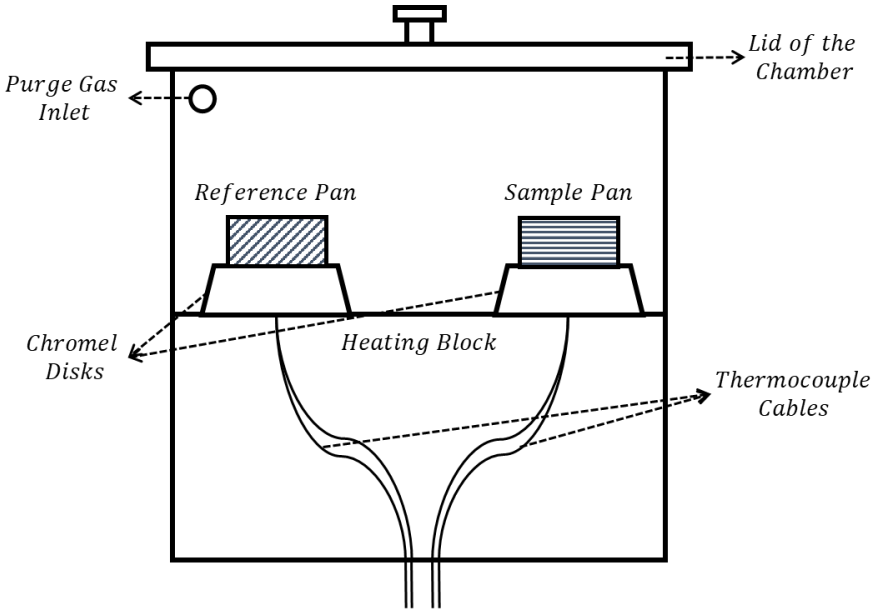

Figure 1.8. Heat flux DSC chamber drawing

The output of the DSC analysis is called a thermogram. An example curve for DSC thermogram is in Fig. 1.9.

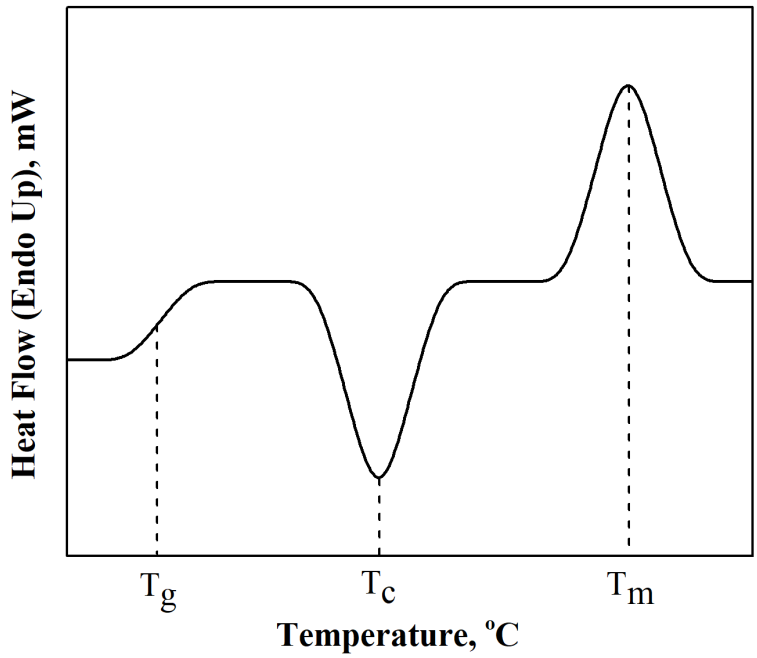

Figure 1.9. An example DSC thermogram; where T_g, T_c and T_m denote glass transition, crystallization and melting temperature values, respectively

Al-Habsi et al. (2013) studied honey crystallization kinetics by DSC. The role of DSC in that study was to measure the melting enthalpy of the crystallized honey. On the other hand, they also measured the crystal content of honey by using high performance liquid chromatography (HPLC) and correlated the melting enthalpy with crystal content to develop a crystal measurement method by DSC. They achieved a high correlation between two methods (R^2=0.99).

1.6.2 Time Domain Nuclear Magnetic Resonance (TD-NMR) Relaxometry

Nuclear magnetic resonance (NMR) relaxometry is a non-destructive and non-invasive tool that gives information about the molecular changes of the interested system. In food science, it has been used in fruit, vegetable, meat, dairy, cereal, and bakery products for quality control and characterization purposes (Kirtil & Oztop, 2016). When conducting an NMR experiment, firstly, protons are aligned in the direction of magnetic field, then radiofrequency (RF) pulse is applied to flip the protons to the perpendicular direction to the magnetic field. When the effect of RF pulse is removed, protons recover their direction to the magnetic field. This is called relaxation. Spin movements with and without a magnetic field is represented in Fig. 1.10.

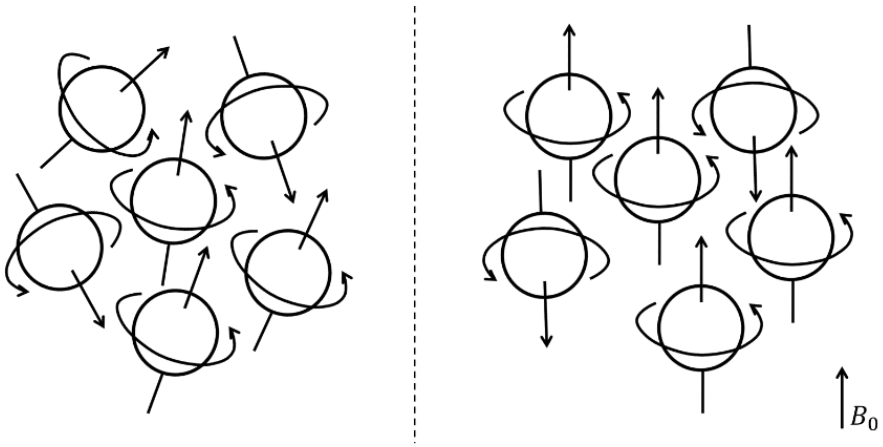

Figure 1.10. Spin rotation without magnetic field (on left) and with magnetic field (on right)

Application of RF pulse flips the spins to the perpendicular plane of magnetic field direction. Spin movement by RF pulse can be seen in Fig. 1.11.

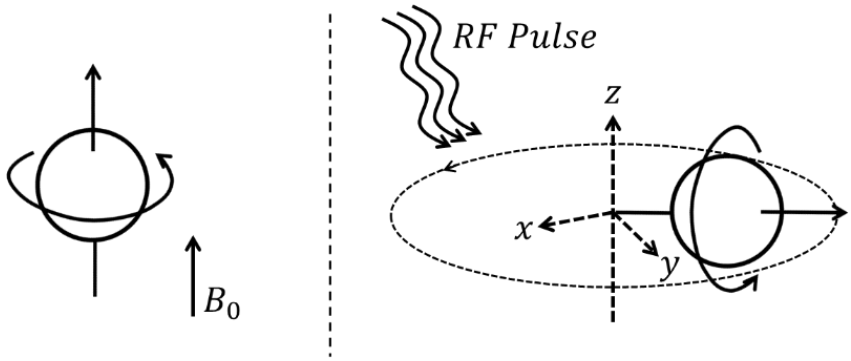

Figure 1.11. Spin alignment under magnetic field (on left) and flipping down to xy-plane by RF pulse (on right)

When the effect of RF pulse is removed, spins turn back to their initial alignment by the magnetic field. This movement is illustrated in Fig. 1.12.

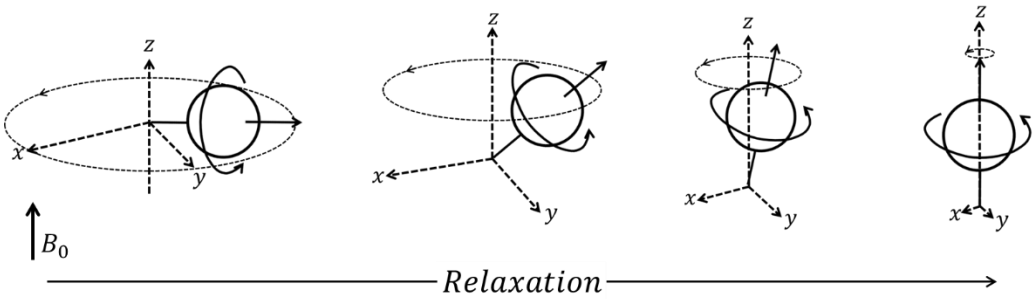

Figure 1.12. Spin movement while relaxation

Time-domain NMR (TD-NMR) techniques are frequently used in polymer, pharmaceutical, and food industries as they offer rapid experimentation and do not require any preliminary sample preparation. Most of the time, proton (^{1}H) NMR is used in TD-NMR experiments. And the relaxation times, T_1 (spin-lattice) and T_2 (spin-spin) are frequently measured to explore the changes and dynamics in the

systems. T_1 relaxation time is a relaxation variable indicating how the net magnetization of the spins are recovering back to the initial spin alignment after RF pulse. T_2 relaxation time is another relaxation variable showing how fast the RF pulse flipped magnitude decays. Representative T_1 and T_2 curves are in Fig. 1.13 and 1.14, respectively.

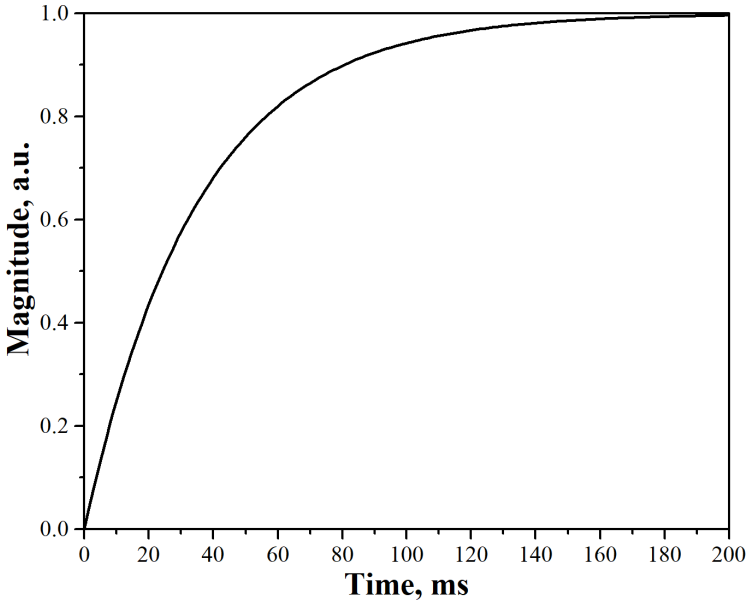

Figure 1.13. Example T_1 recovery curve

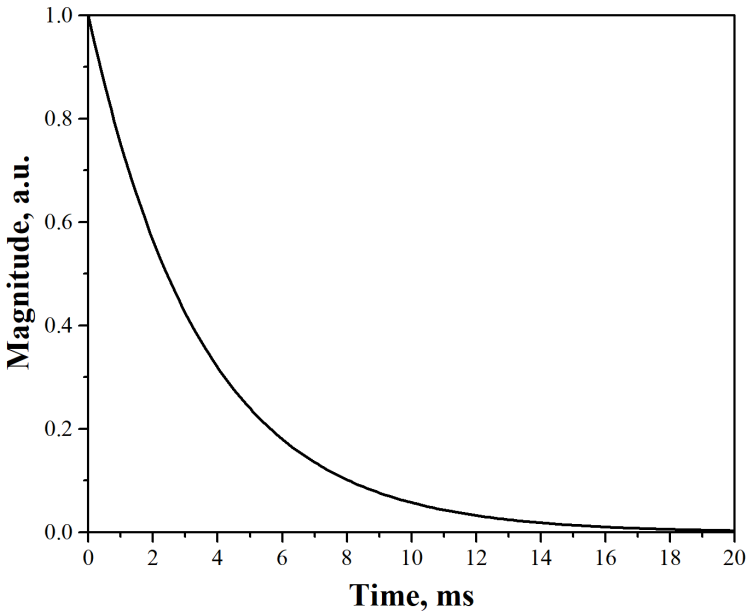

Figure 1.14. Example T_2 decay curve

In the study of Ribeiro et al. (2014), several Brazilian honey samples were examined to detect the botanical origin by low field nuclear magnetic resonance (LF-NMR) experiments. T_2 relaxation times were measured, and results showed the presence of two proton populations in the samples. Similarly, in another study where honey was adulterated with corn syrup, T_2 relaxation decays signals confirmed the presence of two proton populations, and the relaxation times of these proton pools changed with fructose syrup addition (R. D. O. R. Ribeiro et al., 2014). Tappi et al. (2019) investigated the crystallization of honey by using static and dynamic experiments and checked water activity, DSC and also used TD-NMR through T_2 relaxation times and showed that TD-NMR allowed to separately observe the two kinds of protons, both pertaining to liquid sugars, one chemically exchanging with water and one not exchanging with it (Tappi et al., 2019). It was concluded in the study that the interaction between crystals and liquid honey showed some differences according to the type of crystallization process due to the different number and size of the crystals, but further investigation is needed to clarify the process.

In addition to relaxation times, there are other TD-NMR techniques that are also quite applicable to honey. The most important requirement to obtain quantitatively interpretable data with high signal-to-noise ratio from samples with low moisture content (Grunin et al., 2019) such as honey becomes the selection of the appropriate pulse sequence. In such samples, the detection of solid and liquid fractions in a sample can be possible with the Free Induction Decay (FID). Indeed the commonly used solid fat content (SFC) method that has been used in the fat and chocolate industry significantly is based on this sequence (AOCS Official Method Cd 16b-93, 2009a). However, the dead time of this sequence can change between 5-10 μs, and depending on the electronics of the hardware; it could go up to 20 μs. In such a case, it is highly probable that the signal from the solid fraction cannot be detected correctly or at all.

In polymer science literature, to determine the crystalline regions in the solid polymers (Maus et al., 2006); to monitor the kinetics of the crystallization process (Dejong & Hartel, 2016); to obtain quantitative measurement on more mobile amorphous fractions, various NMR approaches have been followed (Grunin et al., 2019). Crystallization kinetics of sorbitol was studied by using TD-NMR in a study (Dejong & Hartel, 2016). Their approach was also based on the measurement of solid fat content, and the NMR pulse sequence used in that study was free induction decay (FID). While using this sequence, due to the dead time, there is a requirement to make the data observed corrected by using a correction factor, F. And this correction factor changes for different instruments and samples. A similar approach was also used in another study to determine the sucrose crystal content in a confectionery product (Porter & Hartel, 2013).

To remove the "dead time" problem of the measurements by FID sequence, another sequence was developed: Magic Sandwich Echo (MSE). By the principle of refocusing to initial part of signal acquired, data from solid portion of the sample can be collected (Grunin et al., 2019). In addition to this, determination of crystalline and amorphous fractions is possible by MSE sequence according to Maus et al. (2006). There are NMR studies by MSE sequence, but mostly about polymer science (Papon et al., 2011; Pieruccini et al., 2015; Sturniolo & Saalwächter, 2011).

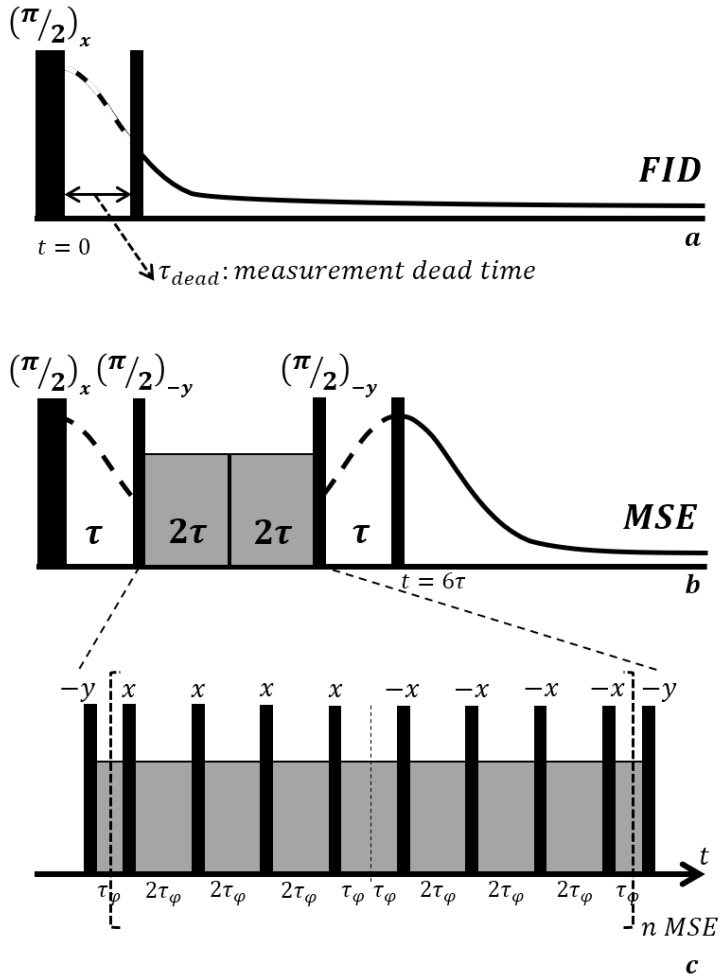

Figure 1.15. Comparison of FID (a) and MSE (b) sequences and MSE sequence pulse diagram (c)

The dead time of FID sequence is given in the Fig. 1.15 (a) and the removal of dead time by MSE sequence is shown in Fig. 1.15 (b).

1.7 Objective of the Study

The first objective of this study is to investigate the crystallization of honey samples induced with seeding by using time-domain nuclear magnetic resonance (TD-NMR) through Magic Sandwich Echo (MSE) pulse sequence and to compare the results with differential scanning calorimetry experiments. To our knowledge, this is the first time where MSE sequence is used to follow crystallization kinetics in honey or in any food system. NMR relaxation times, T_1, and T_2 were measured to make a comparison with the previous studies.

The second objective of this study is to determine adulteration of honey by using TD-NMR techniques through MSE pulse sequence and relaxation time measurements. To our knowledge, this is also the first study where MSE is used to determine adulteration in honey. To determine the properties of the honey and get complementary results for NMR measurements, sugar profile by using high performance liquid chromatography analysis, water content by using Karl Fisher titration and water activity by equilibrium relative humidity experiments were also performed.

The last objective of this study is to examine the crystallinity change of already crystallized honey samples by MSE and to monitor the melting behavior of honey real time by using TD-NMR.

CHAPTER 2

MATERIALS AND METHODS

2.1 Materials

Honeydew honey (pine) was provided from a local producer in Ankara, Turkey. Powder glucose was purchased from Tito (Turkey). Corn syrups were kindly provided by Sunar group (Adana, Turkey). Two type of syrups (SG-60, HFCS-42) of which the composition will be given later was used.

2.2 Characterization of Honey and Syrups

2.2.1 Sugar Composition by HPLC

For the sugar profile, the method described by Namlı (2019) was followed. 1 g of honey and sugar syrups were weighed and dissolved in 50 mL HPLC grade water (Milli-Q Water System, Millipore S.A., France) sample was shook in vortex shaker for 5 mins to ensure complete hydration of honey. The obtained solution was filtered by 0.45 μm nylon filter and introduced to HPLC vial. The instruments used in HPLC system are an HPLC-RID (Shimadzu Scientific Instruments, Japan) with an auto-sampler (SIL-20A HT), degasser (DGU-20A_5), pump (LC-20AD), column oven (CTO-20A) and refractive index detector (RID-20A). Inertsil NH_2 column (Shimadzu Scientific Instruments, Japan) (dimensions of 250x4.6, 5μm) was used. As the mobile phase, acetonitrile and water mixture (80:20 v/v) was driven. Injection volume of the sample and flow rate of mobile phase are 20 μL and 1 mL/min, respectively. Oven temperature was set to 40℃ during separation.

2.2.2 Water Content by Karl Fisher Titration

To determine the water content of honey, Karl Fisher Titrator was used (TitraLab KF1000 Series, HACH, UK). Reaction mechanism occurred in titration cell is the following:

$$R - OH + SO_2 + R'N \rightarrow [R'NH]SO_3R + H_2O + I_2 + 2R'N$$
$$[R'NH]SO_3R + H_2O + I_2 + 2R'N \rightarrow 2[R'NH]I + [R'NH]SO_4R$$

In the product side of the first step of the reaction, water is introduced to the system with the addition of the moist sample. Interaction of elemental iodine with water is represented in the second step of the reaction.
In the second step of the reaction given, there are elemental iodine and ionic iodine. By the potential difference between them, the amount of iodine was calculated and hence the amount of water was determined stoichiometrically. Because the system is based on the electrical potential difference measurement of the ion couples, this is also called coulometric titration.

2.2.3 Water Activity

Water activity measurements were performed at 25℃ by using water activity analyzer (AQUALAB 4TE, METER Group, Pullman, WA). The measurement was done by equilibrium relative humidity method. This method is based on the measurement of the relative humidity of the air that is equilibrated with the sample in terms of thermodynamic properties. It was assumed that the relative humidity of the air in the measurement chamber represents the water activity of the sample.

Results of the composition analysis and physical properties are given in Table 2.1.

Table 2.1 Physical properties and composition of the used honey sample and syrups

	Honey	**HFCS**	**GS**
Water Activity* (α_w)	0.5721± 0.0054	0.7265± 0.0018	0.6484± 0.0094
Water Content* (g/100 g)	15.3056± 0.0616	23.9333± 0.3429	16.3696± 0.0590
Fructose (g/100 g)	34.3022	28.8932	0.4838
Glucose (g/100 g)	28.5447	38.2311	24.9697
Maltose (g/100 g)	10.4752	2.9101	31.6716
DP3**(g/100 g)	0.0000	0.9081	9.2341
DP4** (g/100 g)	9.8438	0.0000	0.0000
DPn** (g/100 g)	0.2342	0.5577	15.6308

**Water activity and water content data were reported as the mean values of at least 3 replicates and their corresponding standard deviations.*
***DP_3 and DP_4 denoted sugars consisting of 3 and 4 monosaccharides, respectively and DP_n denoted the remaining sugars.*

2.3 Sample Preparation for Crystallization and Melting Experiments

White et al. (1962) showed that crystallization was accelerated when glucose to water ratio was higher than 2.10. As given in Table 2.1, it was observed that the initial ratio of glucose to the water of the honey sample was 1.92, which indicated that the selected honey sample would not crystallize quickly. Therefore, to accelerate the process, glucose powder was added to the honey sample at a percentage of 5%. Honey was first preheated up to 50°C before seeding to remove the crystal memory. Once glucose was added, it was mixed slowly until a homogenous mixture was obtained. After the addition, the glucose to water ratio became 2.25, and crystallization was triggered.

2.4 Sample Preparation for Adulteration Experiments

So as to adulterate honey; high fructose corn syrup (HFCS) and glucose syrup (GS) were used. They were mixed with honey individually at 2,5, 10, 15, 20, 25, 30, 40,

50% percentages. Mixtures obtained were heated up to 50℃ to remove the crystal memory of samples and stirred continuously to provide homogeneity among all samples. Honey samples were put to the 10 mm NMR test tubes and measurements were conducted when temperature equilibrated to 28℃ *(actual working temperature of the NMR system).*

2.5 Differential Scanning Calorimetry Experiments (DSC)

DSC 4000 (Perkin Elmer, MA, USA) was used to determine the melting enthalpy of the crystallized honey. The flow rate of the nitrogen gas to the system was set to 19.8 ml/min. The samples were put in hermetically sealed aluminum pans at about 25 mg of sample load. Samples were directly heated from 20℃ to 100℃ at a rate of 5℃/min. From initial seeding, at every 12^{th} hour, measurements were recorded. To examine the peak area of the thermogram, Pyris Manager software was used.

2.6 Time-Domain Nuclear Magnetic Resonance (TD-NMR) Experiments

TD-NMR experiments were performed using a 0.48 Tesla (^{1}H frequency of 20.34 MHz) NMR System (Spin Track, Resonance Systems GmbH, Kirchheim/Teck, Germany) equipped with a 10 mm radiofrequency (RF) coil. Samples were put to tubes corresponding to a sample of the height of 1.5 cm. Tubes were closed with a lid and stored in an incubator at 14℃ (DAIHAN Scientific, DKSH Group, Philippines) for crystallization. Crystallization measurements were done in NMR right after the samples were removed from the incubator. The temperature difference during that period was neglected. Crystallization was monitored for 96 hours for 12h intervals. Adulteration measurements were performed when the tube temperature reached 28℃.

2.6.1 Relaxation Time Measurements

Relaxation times of T_1 and T_2 were measured using *Saturation recovery* and CPMG pulse sequences, respectively. For T_1 experiments, delay time changed between 3-200 ms for 32 points with a repetition delay of 1s and 4 scans. For T_2 experiments, 64 echoes were used with an echo time of 300 μs, the repetition delay of 1 ms, and 32 scans. 90^o pulse duration was 3.40 μs for the coil. T_1 data were analyzed using MATLAB (MathWorks, 2019) by fitting the data to a mono-exponential model (R^2>0.99). For T_2 data, a two-component model fitted better, and Relax 8 software was used for the analysis (Resonance Systems GmbH, Kirchheim/Teck, Germany).

2.6.2 Crystal (Solid) Content Measurement

Magic sandwich echo (MSE) sequence was used to estimate the crystal content. The system was operated at 28℃. Pulse diagrams and the working principle of the pulse sequences are explained in the study of Grunin et al. (2019). Repetition time and the number of scans were set to 10,000 ms and 16. A plot of a representative signal of the MSE sequence is given in Fig. 2.1 and a representative magnitude data are presented. To calculate the crystallinity, the magnitude of the signal was calculated first, and the following ratio was calculated:

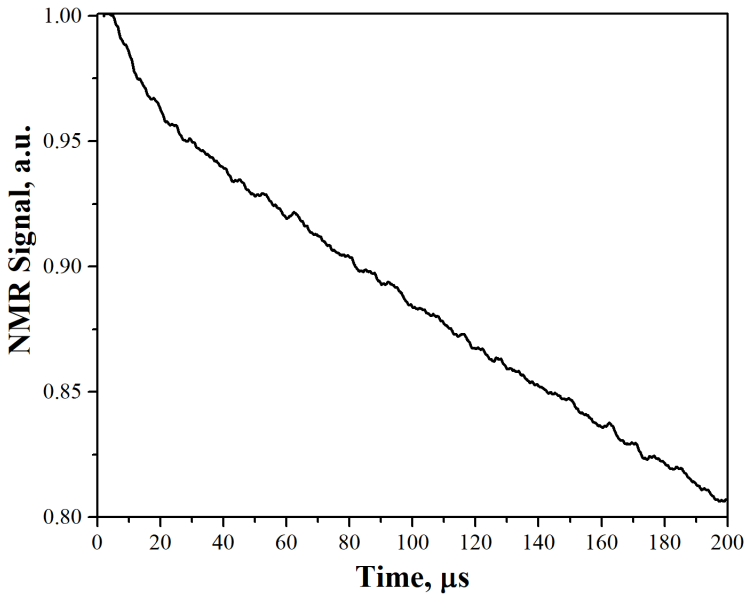

Figure 2.1. A representative NMR signal from the MSE pulse sequence

$$NMR\ Value = \frac{Magn_{Short} - Magn_{Long}}{Magn_{Short}} \times 100 \quad \textbf{(Eqn. 1)}$$

$Magn_{short}$ denotes the average signal coming from the solid and liquid portion, whereas $Magn_{long}$ denotes the liquid signal only. $Magn_{short}$ covered the average of the data between **2.5-11** μs, whereas for $Magn_{long}$ data, between **100-150** μs was used. NMR value, which is actually a '**%**,' was used as a relative value for the % crystal content.

2.6.3 Melting

For the melting part of the study, already crystallized honey from the first part of the study was used. Samples were placed into the TD-NMR system that was set to 50°C, and the MSE sequence was operated at '*auto measurement mode,*' which consisted of 32 seconds waiting time between measurements for 800 seconds of total experiment time.

2.7 Statistical Analysis

Analysis of Variance (ANOVA) was used to find out the differences (Minitab Inc., Coventry, UK). Tukey's comparison test at 95% confidence interval was used for pairwise comparisons.

Pearson correlation analysis was conducted between 204 NMR and DSC results using MINITAB (Version 19, U.K). Analysis was based on at least 3 replicates for each sample. Both correlation coefficients and p values were reported at a significance level of 5%.

2.8 Experimental Design

The parameters and the testing levels for each factor and the measured responses are summarized in Table 2.2, Table 2.3, and Table 2.4.

Table 2.2 Experimental design table for crystallization

Sample	Storage Temperature (℃)	Measurement Time (h)	Measurements
Glucose seeded honey	14	0, 12, 24, 36, 48, 60, 72, 84, 96	Water content DSC HPLC TD-NMR: MSE TD-NMR: T_1 TD-NMR: T_2

Table 2.3 Experimental design table for adulteration

Sample	Adulteration Percentage (%)	Analyzes
Honey/Glucose syrup	0, 2, 5, 10, 15, 20, 25, 30, 40, 50, 100	Water content Water activity Total soluble solid HPLC TD-NMR: MSE TD-NMR: T_1 TD-NMR: T_2
Honey/HFCS		

Table 2.4 Experimental design for melting

Sample	Measurement Period (s)	Measurement Interval (s)	Temperature (℃)	Analyzes
Crystallized Honey	800	32	50	TD-NMR: MSE

CHAPTER 3

RESULTS AND DISCUSSION

This section was reported in three parts in accordance with the experimental design as: crystallization, adulteration, and melting.

3.1 Crystallization Experiments

3.1.1 DSC Experiments

The result obtained from DSC analysis to observe crystal content change showed that the rate of crystallization was proportional to the amount of uncrystallized honey before 60 hours (Fig. 3.1). And it seemed that it would follow a T_1 '*recovery like*' exponential behavior.

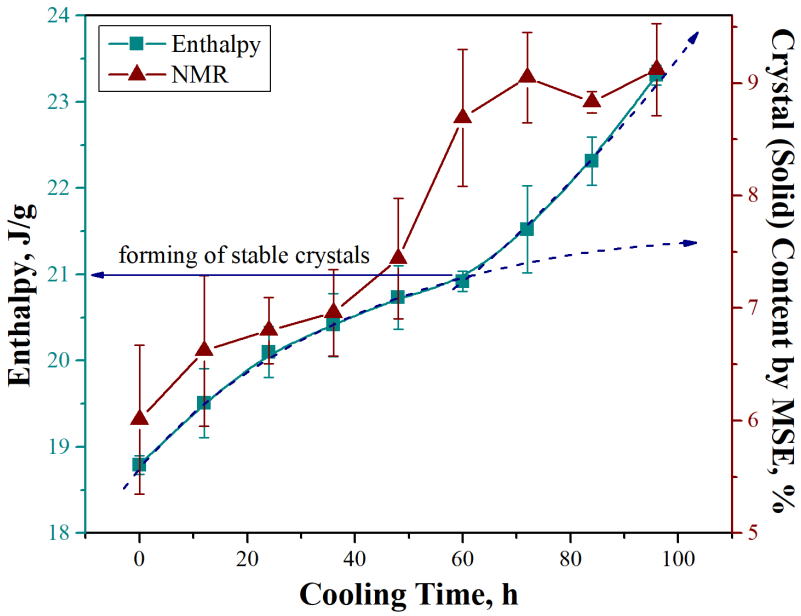

Figure 3.1. Change in the crystal melting enthalpy (by DSC) and crystal (solid) content by MSE experiments

Eqn. 2 shows the mathematical expression of this behavior and indicates the mass of crystal that is valid for the time interval of the first 60 hours.

$$m_{cr}(t) = m_0(1 - e^{-t/\tau_{cr}}) \quad \textbf{(Eqn. 2)}$$

Where m_0 is the total mass of the sample, τ_{cr} is a time characterizing the crystallization rate and could depend on temperature, number of crystallizing nuclei, and physical chemistry of the honey used. In mathematical manner, τ_{cr} is the time at which 63.21% of the maximum amount of crystal is formed. Since enthalpy measured for melting must be proportional to the amount of crystallized honey, the trend of these outputs of DSC can be correlated with the mass of the crystalline portion. As seen in the enthalpy curve of Fig. 3.1, the trend of the development of the curve (*line with the arrow*) can be explained with the model described in the Eqn. 2. m_{cr} (*2.65*) indicates the amount of crystal in the sample and τ_{cr} (*36.45 h*) is the time constant. Such a high relation (R^2>0.98) confirmed that crystal melting enthalpy could be directly correlated with the amount of crystal, up to the point where stable crystals will be formed, and crystallization kinetics depended on the mass of uncrystallized honey. In the study conducted by Al-Habsi et al. (2013), the amount of crystal portion of the honey was stoichiometrically calculated and correlated well (R^2=0.99) with the crystal melting enthalpy change. Here we directly used the change in enthalpy with respect to time.

However, that exponential trend changed after some point. From about 60 hours, an abrupt change was observed on the data. This change occurred near the inflection point of the enthalpy data as 21 J/g and attributed to the formation of larger crystals (Fig. 3.1). It was hypothesized that after this point, the higher energy requirement was not due to the increasing amount of crystal but instead the increasing bonding within the merged grown crystals. In other words, the energy required to melt larger and smaller crystals is different.

In the studies covering a more extended period (up to 2 months) of crystallization, after a linear period, a region of the plateau was also observed, indicating the maximum crystal amount in the honey (Tappi et al., 2019). For this study, such a plateau was not observed for 96 hours.

3.1.2 Time Domain Nuclear Magnetic Resonance (TD-NMR) Experiments

3.1.2.1 Relaxation Time Measurements

Relaxation times of the glucose seeded honey samples were measured during crystallization. T_1 relaxation times fitted to a single exponential and did not show a significant change during that period (Fig. 3.2). The study of Płowaś-Korus et al. (2018) showed that 20 MHz of Larmor frequency was the most insensitive to T_1 NMR relaxometry for determination of changes in the honey, so that was consistent with our findings.

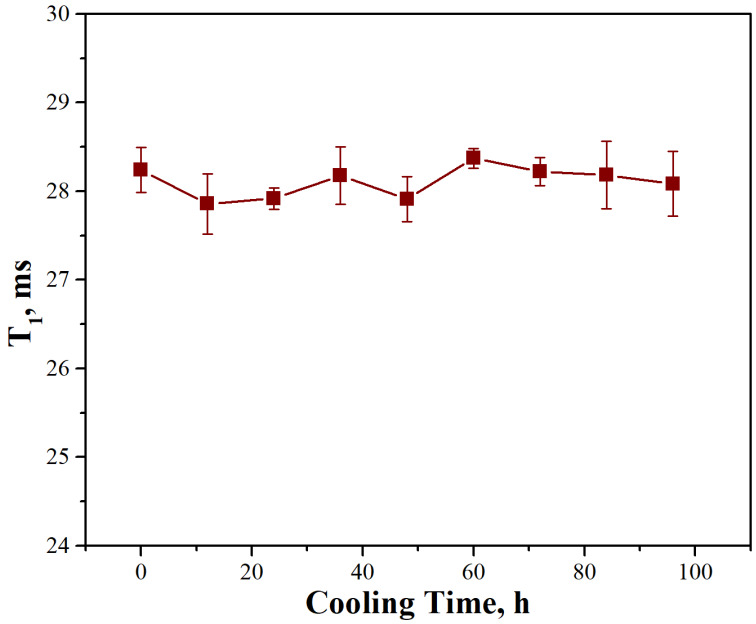

Figure 3.2. Change in T_1 relaxation time during crystallization

From the CPMG (T_2 relaxation) experiments, 2 proton pools were detected as in the study of Ribeiro et. al (2014). The relaxation times of these proton pools were referred to T_{21} (*long*) and T_{22} (*short*) and their contribution to the signal was expressed as A_{21} and A_{22}. A representative relaxation spectrum showing the proton pools is given in Fig.3.3 and change in the relaxation times of these proton pools is given in Fig. 3.4.

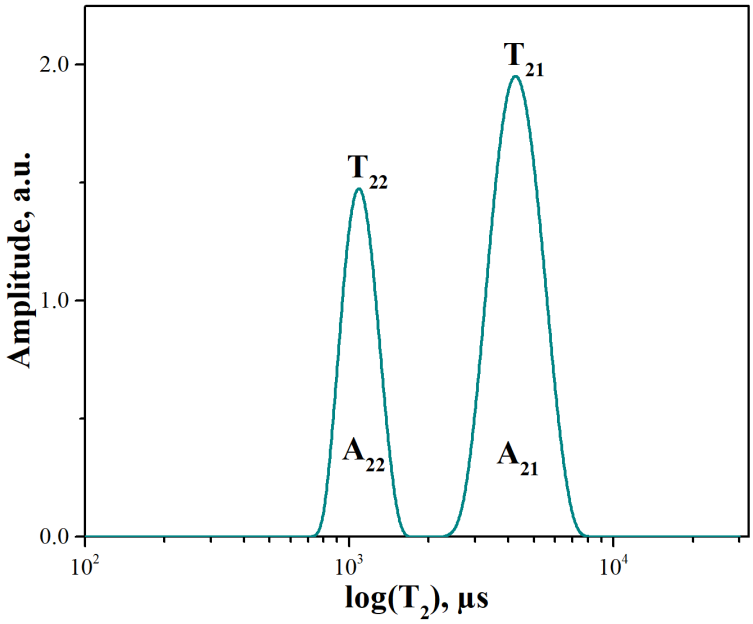

Figure 3.3. A representative T_2 relaxation spectrum showing the multiexponential nature of honey

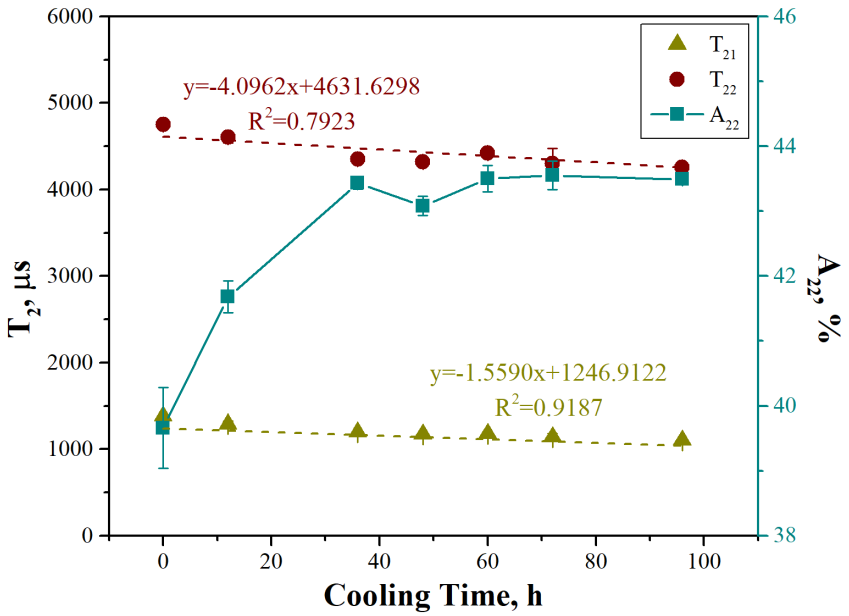

Figure 3.4. Change in T_2 relaxation times and the contribution of the 2nd proton pool (A_{22}) to relaxation during crystallization

Both component's relaxation times decreased with an increase in crystallization. It was not possible to detect the glucose crystals and attribute any of these components to the crystals directly since the echo time used was 300 µs, which was longer than sugar crystal's T_2 relaxation. Also, there was the dead time of the probe that was around 9 µs. However, despite the echo time being used was longer than the one used in the study of Tappi et al. (2019), the relaxation times obtained were in the same range. They attributed the proton pools to exchangeable and non-exchangeable proton populations. Water and labile sugar protons can be considered exchangeable proton pools (Petracci et al., 2014; Tappi et al., 2019). The remaining sugar protons which were bound, and the non-labile –OH protons that could not exchange with water could be considered as non-exchangeable pools. Both proton pools showed a decreasing trend on the relaxation times as crystallization occurred (T_{21} and T_{22}), whereas the contribution of the non-exchanging pool increased with crystal content (A_{22}). The decrease in relaxation times could have been associated with reduced mobility. As crystallization proceeded, less effective sugar water exchange took place, and that was reflected as a higher decrease in T_{21}. As stated by Tappi et al.

(2019), with crystals growing, the liquid-solid interface local gradients of the magnetic fields form and led to shorter T_{22} values.

The relation between the T_2 relaxation times in the form of relaxation rate (R_2) and crystal melting enthalpy was also given in Fig. 3.5a-b for both long and short components of the CPMG decay.

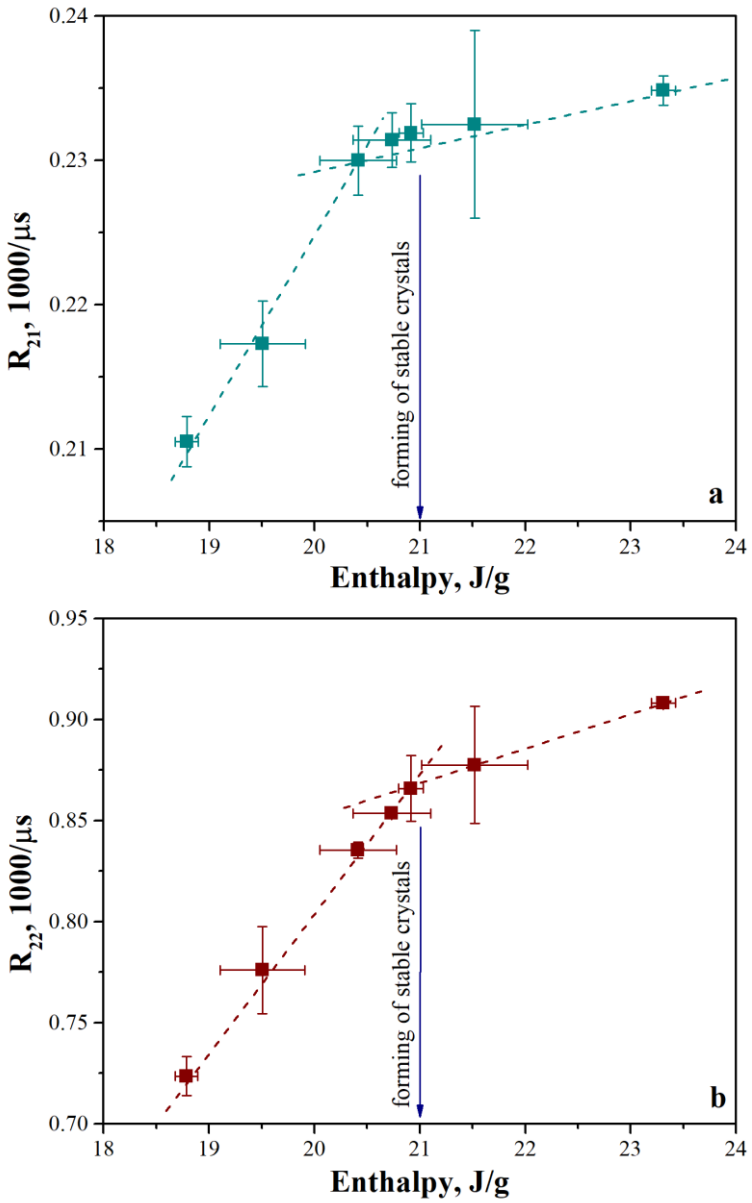

Figure 3.5. Spin-spin relaxation rate of the longer component (a) and the shorter component (b) of CPMG decay vs. melting enthalpy

Rather than T_2, the spin-spin relaxation rate ($R_2=1/T_2$) was used in these plots. As stated before, 2 proton pools have been identified. A_{22} denoted the fraction of liquid located near the crystal surface (interface) and A_{21} denoted the liquid part in free volume (bulk) with corresponding relaxation rate parameters of $R_{21} = (T_{21})^{-1}$ and $R_{22} = (T_{22})^{-1}$. An interesting behavior was observed in these plots. As explained

in Fig 3.1, the signs of the '*crystal size increase*' rather than the amount caused the slope to change in the liquid phase.

It is hypothesized that, at the enthalpy of 21 J/g, merging of smaller crystals into larger crystals occurred, and this was reflected as slope changes in Fig. 3.5a and 3.5b as the deceleration of crystal growth. In Fig. 3.6, it is seen that A_{22} stopped growing fast at melting enthalpy of 21 J/g, which corresponded to crystallization time of 60 hours.

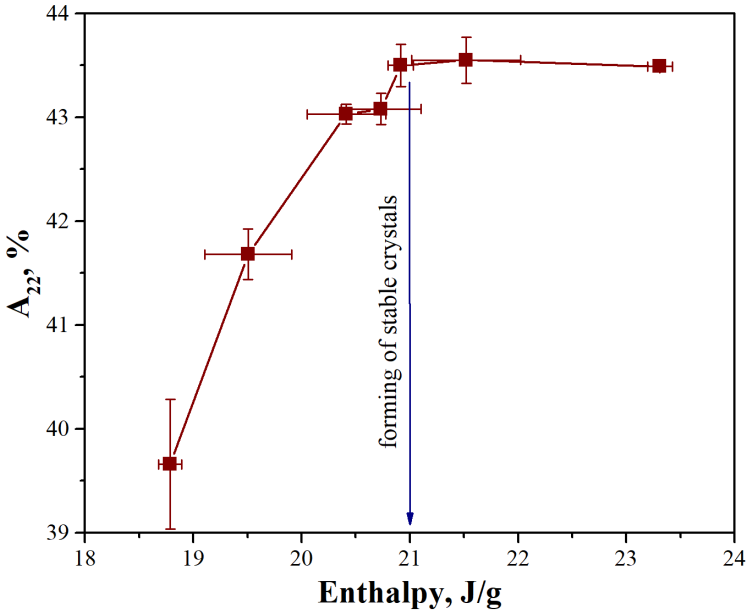

Figure 3.6. Contribution of the faster relaxing liquid into CPMG decay vs. melting enthalpy

The spin-spin relaxation behavior of the liquid phase must be considered more thoroughly. Both two CPMG components were exponential, and this meant the fast exchange of magnetizations between interface and bulk phases. At the same time, the entire relaxation curve consisted of the two components with really different T_2 times, and this unambiguously tells about *two different types of liquid*. These two liquids do not have magnetization exchange, and they both are influencing by the

growing crystals, i.e., they both contact crystals. While conditioning right after a sample reaches 21 J/g melting energy, the ratio between these liquids content stopped changing.

3.1.2.2 Crystallization Estimation through MSE Experiments

As stated before, solid content measurement by MSE was run for 96 hours on glucose seeded honey samples, and data were acquired every 12 hours. Crystal contents obtained through the Eq. 1 from the MSE sequence is given in Fig. 3.1.

Besides, the relationship between DSC and NMR experiments (CC) was also sought for, and the results are given in Fig. 3.7. A significant relation (*also confirmed by Pearson correlation tests; Table 3.1*) was observed between NMR values and DSC results ($r=0.87$, $p<0.05$).

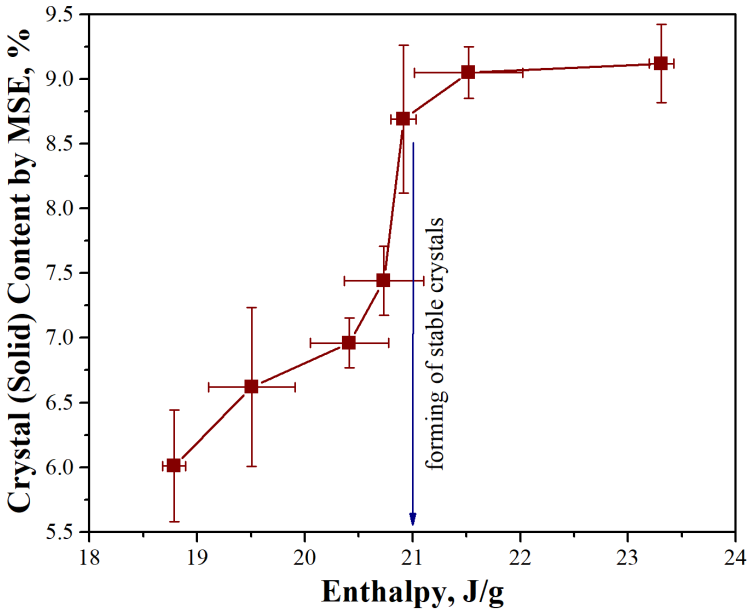

Figure 3.7. Crystal (solid) content by MSE vs. Melting enthalpy

Table 3.1 Pearson correlation analysis between T_{21}, T_{22}, A_{21}, and % crystal content (CC) obtained from MSE experiments

Response1	Response2	Correlation	95% CI for ρ	P-Value
T_{22}	Time	-0.945	(-0.992, -0.667)	0.001
T_{21}	Time	-0.880	(-0.982, -0.377)	0.009
A_{22}	Time	0.750	(-0.008, 0.960)	0.052
CC	Time	0.931	(0.593, 0.990)	0.002
DSC	Time	0.978	(0.857, 0.997)	0.000
T_{21}	T_{22}	0.978	(0.856, 0.997)	0.000
A_{22}	T_{22}	-0.901	(-0.985, -0.460)	0.006
CC	T_{22}	-0.839	(-0.976, -0.232)	0.018
DSC	T_{22}	-0.919	(-0.988, -0.538)	0.003
A_{22}	T_{21}	-0.914	(-0.987, -0.517)	0.004
CC	T_{21}	-0.719	(-0.955, 0.073)	0.068
DSC	T_{21}	-0.857	(-0.979, -0.293)	0.014
CC	A_{22}	0.660	(-0.185, 0.944)	0.107
DSC	A_{22}	0.694	(-0.124, 0.950)	0.084
DSC	CC	0.866	(0.326, 0.980)	0.012

A correlation analysis was also conducted between the relaxation times and the signal obtained from MSE. Pearson correlation results are all given in Table 3.1. As seen in Table 3.1, the correlation coefficient between T_{21} and MSE results (CC values) was quite high ($r>0.84$) and significant ($p<0.05$) supporting the hypothesis that the change in relaxation times of the non-exchanging proton was governed by the increase in the crystal contents.

To our knowledge, there has been no study so far that aims to measure the crystal content of honey by using the magic sandwich echo sequence. Even with the simplest sequence that is FID, such a study does not exist. So, in this study, it was shown that the MSE sequence had great potential to be used for determining the crystallization kinetics. Also, results were very well correlated with DSC results, and the TD-NMR

approach utilized in the study is a much easier and shorter experiment to conduct compared to DSC.

When the MSE output was analyzed with respect to the melting enthalpy, it was observed that both by MSE and enthalpy, the formation of stable crystals with bigger dimensions occurred at 60h. Very likely, it is the fusion of smaller crystals – their amount increased by about 50% (from 7 to 9 by MSE). This is also observable in the enthalpy curve as the inflection point around 21 J/g. The continuation of storage at 14°C did not make a considerable increase of crystals amount (Fig. 3.1 and Fig. 3.7), but assuming that the melting energy is going higher, one can suppose the formation of more intense bonding within the merged grown crystals.

3.2 Adulteration Experiments

3.2.1 Effect of HFCS addition on the T_1 and T_2 relaxation times

Relaxation times of honey samples were measured with respect to adulteration level by HFCS and GS. Fig. 3.8 shows the changes in T_1 and T_2 curves of honey samples adulterated with HFCS.

Table 3.2 Physical properties of HFCS and GS adulterated samples*

	HFCS Adulteration						GS Adulteration					
Adulteration Level, %	**MC, %**	**TSS, °Brix**	**Glu, g/100g**	**Fru, g/100g**	**Mal, g/100g**	**G/W Ratio**	**MC, %**	**TSS, °Brix**	**Glu, g/100g**	**Fru, g/100g**	**Mal, g/100g**	**G/W Ratio**
0.00	15.3056	82.93	28.54	33.30	10.48	1.8647	15.3056	82.96	28.54	33.30	10.48	1.8647
2.00	15.4885	82.69	28.74	33.21	10.32	1.8559	15.3292	82.95	28.46	32.57	10.95	1.8567
5.00	15.7479	82.34	29.03	33.08	10.09	1.8439	15.3594	82.93	28.36	31.64	11.55	1.8465
10.00	16.1693	81.79	29.51	32.86	9.72	1.8251	15.4129	82.90	28.18	29.99	12.62	1.8284
15.00	16.5950	81.22	29.98	32.64	9.35	1.8071	15.4650	82.87	28.00	28.39	13.65	1.8110
20.00	17.0237	80.66	30.47	32.42	8.97	1.7899	15.5219	82.84	27.81	26.63	14.79	1.7921
25.00	17.4744	80.06	30.97	32.19	8.57	1.7727	15.5761	82.81	27.63	24.96	15.86	1.7742
30.00	17.8915	79.51	31.44	31.98	8.21	1.7576	15.6200	82.78	27.48	23.60	16.74	1.7598
40.00	18.7507	78.38	32.41	31.54	7.45	1.7285	15.7293	82.72	27.12	20.23	18.91	1.7243
50.00	19.6036	77.25	33.36	31.10	6.71	1.7022	15.8343	82.66	26.77	16.99	21.01	1.6907
100.00	23.9333	71.53	38.23	28.89	2.91	1.5976	16.3696	82.36	24.97	0.48	31.67	1.5259

**Parameters at different adulteration levels were calculated by a sample mass balance based on the information in Table 2.1*

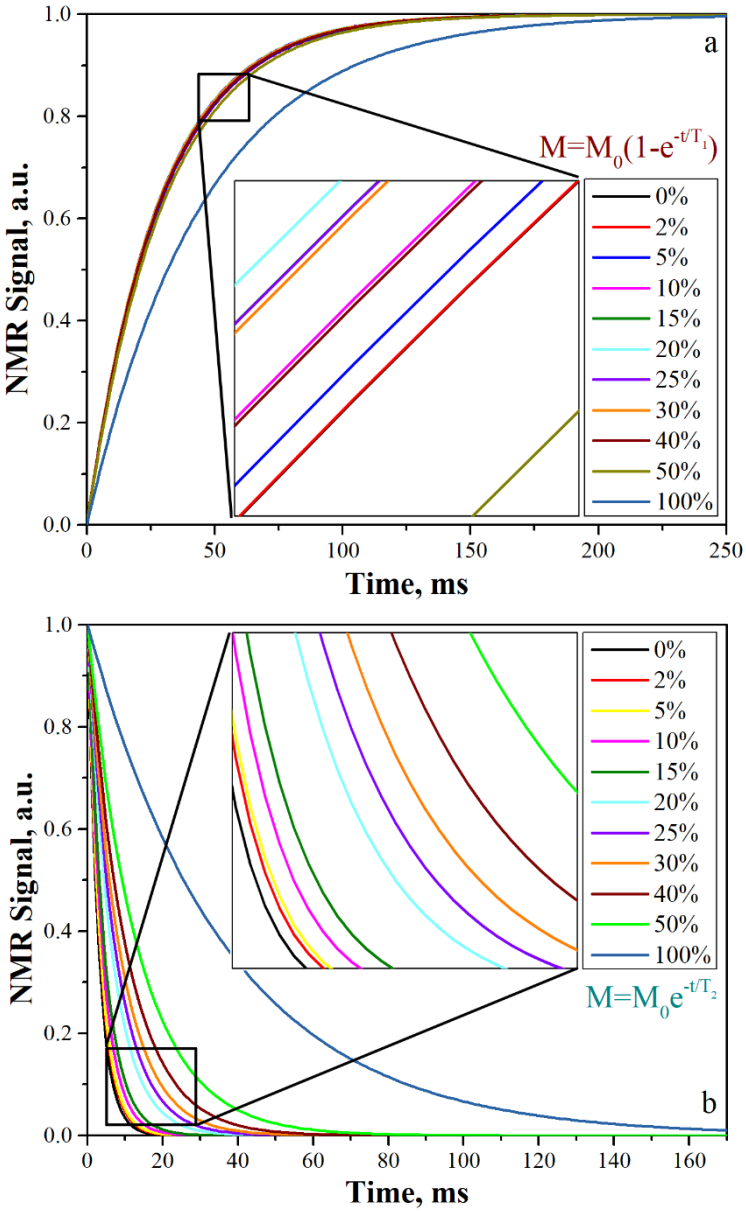

Figure 3.8. T_1 recovery (a) T_2 decay curves (b) of samples adulterated by HFCS

It can be seen that as HFCS was added to the honey, relaxation slowed down. In other words, addition of HFCS increased the T_2 times of honey significantly ($p<0.05$). The T_2 relaxation decays of adulterated samples were fitted to both mono-exponential (T_2) and bi-exponential models (T_{21}, T_{22}) and resulting relaxation times are shown in Fig. 3.9 with respect to the adulteration level.

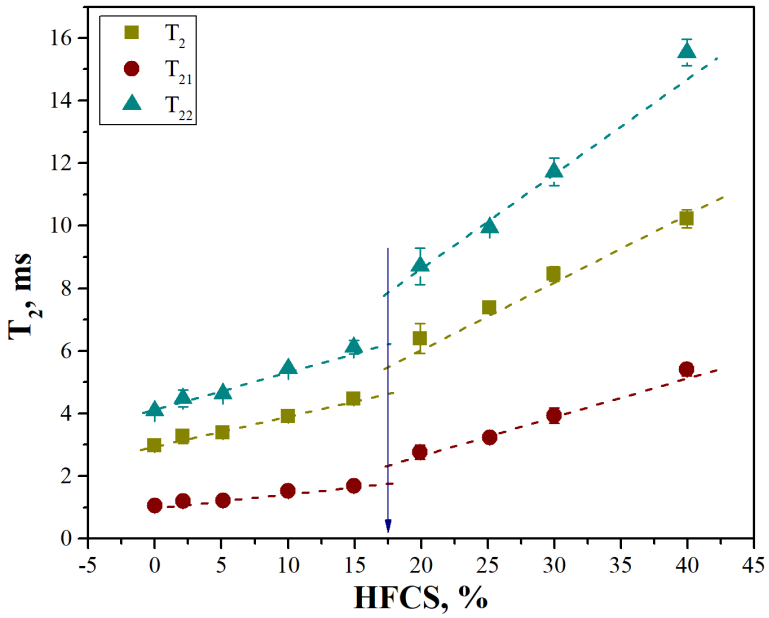

Figure 3.9. T_2 values of HFCS adulterated samples

As given in Table 2.1, HFCS had a higher water content (~23%) and water activity (~0.73) than honey (~15%, ~0.57). Thus with the addition of HFCS, an increase in relaxation times was expected (R. D. O. R. Ribeiro et al., 2014) and this was the observed case shown in Fig 3.9.

When the T_2 decays were decomposed, two proton pools were detected. The faster relaxing component (T_{22}) was associated with the liquid located near the solid portion and increased with HFCS addition. Besides this, the slower relaxing component (T_{21}) that was associated with the liquid in bulk portion increased with increasing water content. Fast component was more affected from HFCS addition as the slope increased almost 3 folds while it was 1.5 for the slow relaxing component. Pearson correlation coefficients between HFCS content and both T_2 times were found be significant ($p<0.05$) and quite high ($R>0.83$).

For T_1 recovery curves a mono exponential model was used. However, for T_1 times, an interesting case was observed on the dependence of relaxation times with respect to HFCS content (Fig. 3.10). Up to a certain adulteration level, relaxation times

decreased slightly, and this was statistically significant ($p<0.05$). It was also interesting to see that at that concentration; dependence of HFCS to T_2 times changed its slope.

As seen from the composition of HFCS (Table 2.1); syrup mostly consisted of fructose and glucose and slight amount of maltose (~3%). With increasing water content in honey viscosity is also affected and it decreases (Yener et al., 1987). Decreasing viscosity implies more mobility and this is directly reflected in the relaxation times. However, for T_1 relaxation this is not always the case. T_1 is the shortest when the molecular tumbling rate (also known as the correlation time τ_c), is approximately equal to the Larmor frequency. Molecules tumbling faster or slower are less efficient at spin-lattice relaxation and have longer T_1s. Free water or crystals (Le Botlan et al., 1998) have longer relaxation times due to the wide range of tumbling rates and so most molecules in this state are inefficient at T_1 relaxation. The change in T_1 of honey could also be attributed to the change in the correlation times. With increasing HFCS, correlation times could have decreased and so decreased the T_1 relaxation. However, after 20%, water started to dominate and increased the relaxation times (Fig. 3.10).

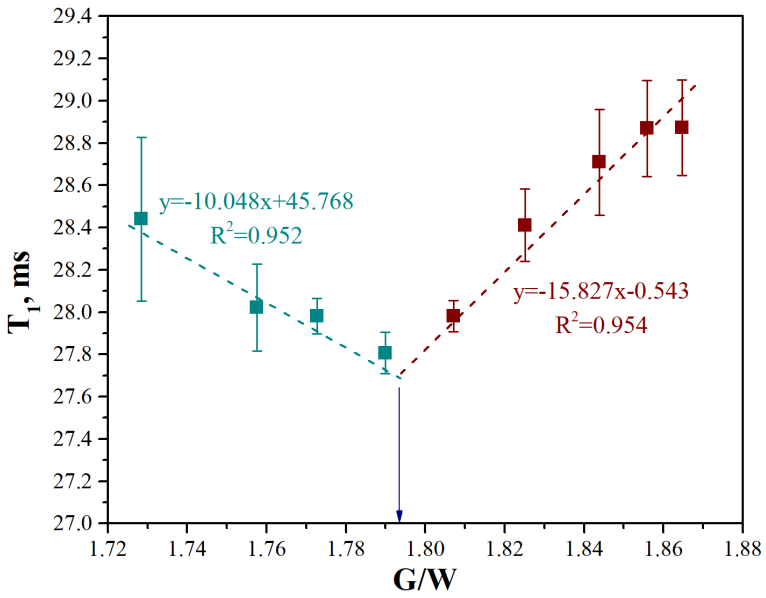

Figure 3.10. T_1 values of HFCS adulterated samples

T_2 relaxation times were also affected from this change and a slope change was observed with respect to HFCS addition. As stated before, fast relaxing component was affected more. This is probably due to fact that additional water had the tendency to hydrate the solid portion first and more and thus decreased the relaxation rate.

3.2.2 Effect of GS addition on the T_1 and T_2 relaxation times

Glucose syrup was also added to the honey at the same concentrations and changes in relaxation time were observed (Fig 3.11a-b).

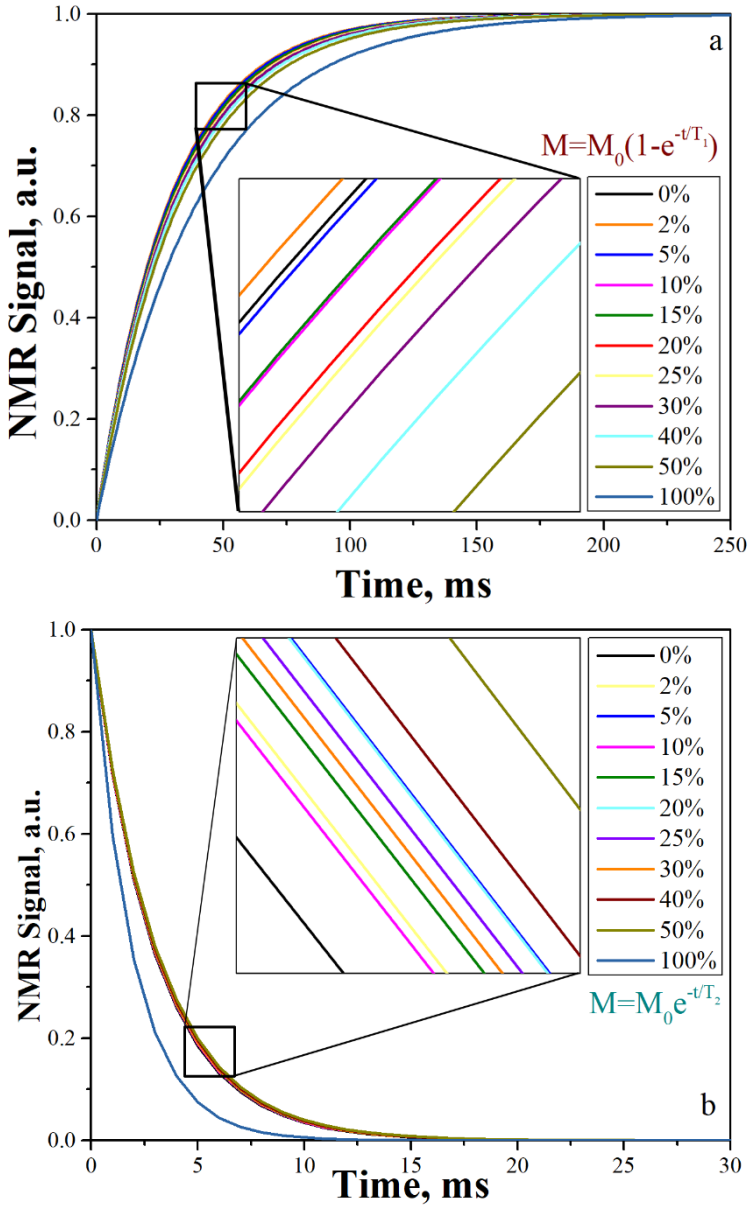

Figure 3.11. T_1 recovery curves (a) T_2 decay curves of samples (b) adulterated by GS

Different from HFCS, GS had a significant amount of trisaccharide (DP_3~9%) and higher order polysaccharides (DP_n~16%). Water activity was higher (~0.64) than honey but water content was close (~16%). The maximum amount of GS addition; that is 50% increased the water content just by 0.5%. It is known that higher

molecular weight sugars increase viscosity. Thus, in polymer systems, increased viscosity can decrease relaxation times as they are expected to decrease the mobility of free water (Kruk et al., 2012).

Water content of the honey samples adulterated with GS did not increase too much but water activity increased. Increase in water activity was reflected as an increase in T_1 (Fig. 3.11a). A significant ($p<0.05$) and very high positive correlation was detected between the a_w and T_1 of honey samples ($r=0.950$). Less hydration ability of the higher molecular weight sugars compared to monosaccharides might have resulted in skipping of the 'T_1 decrease' region which was observed in HFCS added samples.

T_2 relaxation times of GS adulterated honey samples were also examined. Both mono and biexponential analysis were conducted. Mono exponential T_2 values did not show a good correlation with increasing GS content ($R^2=0.515$). In addition, no change was observed in the T_2 of slow relaxing component ($p>0.05$). That was not unusual as the bulk water content did not increase significantly. However, the fast-relaxing component's T_2 values decreased with increasing GS concentration (Fig. 3.12b).

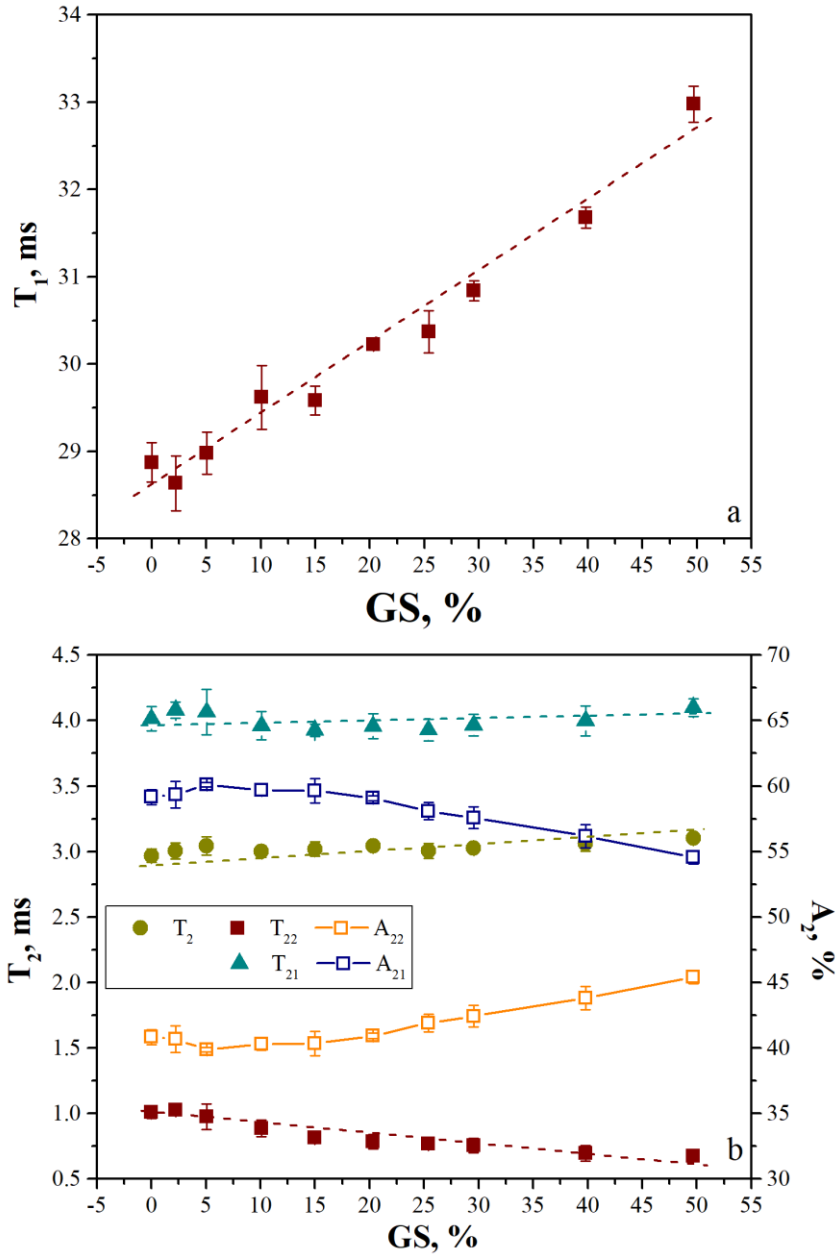

Figure 3.12. T_1 values of GS adulterated samples (a) mono and bi-exponential fitting results of T_2 times (b)

As stated before, the fast component was associated with the protons associated with the sugars. As GS was added, high molecular weight polysaccharides contribution increased which induced a decreased mobility and that could have resulted in shorter

T_2 for the fast-relaxing component. Therefore, it is also possible to state that contribution of the higher molecular weight sugars to the bulk viscosity seemed not significant in this case. Increase in T_1 values also confirmed this finding.

3.2.3 Use of Magic Sandwich Echo (Pulse) Sequence to Investigate Adulteration

Magic sandwich echo (MSE) is a specialized solid echo pulse sequence and involves a phase cycling step different than Solid Echo (SE). Details of the sequence can be found in previous studies (Grunin et al., 2019; Maus et al., 2006). The information obtained from MSE is similar to the conventional FID sequence which has commonly been used to measure solid fat content (SFC) in food samples (AOCS Official Method Cd 16b-93, 2009b). In this study, it has been used to differentiate the signal coming from the solid and liquid portions of honey and how they were changing with respect to different adulteration levels. Since the calculation involved the quantification of 'solid' portion the measured parameter was defined as 'Crystal Content%'. Results of the CC% are given in Figure 3.13.

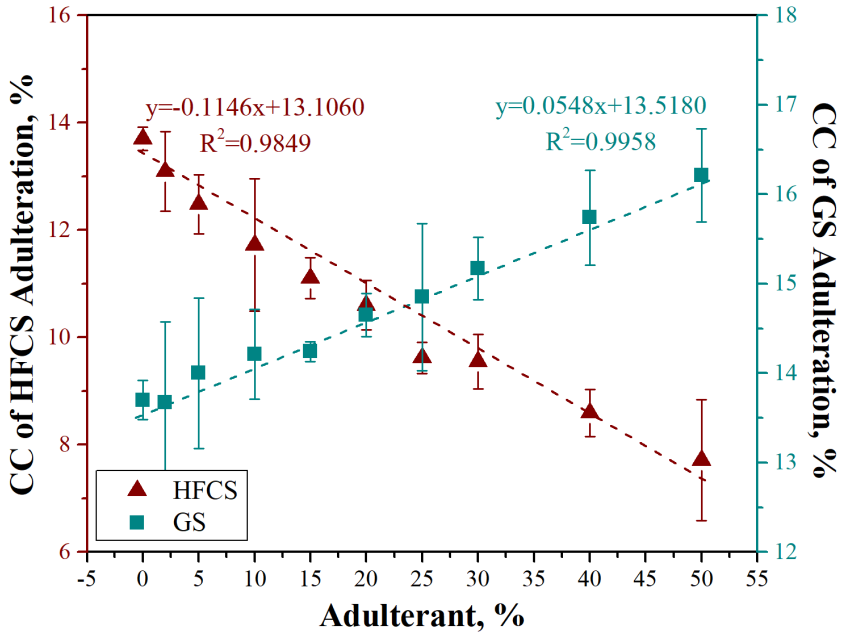

Figure 3.13. MSE values of HFCS and GS adulterated samples with respect to adulteration level

CC% values decreased with HFCS addition and increased with GS addition. A significant ($p<0.05$) and high negative correlation was detected ($r=-0.944$) between HFCS% and CC%. Increase in water content was a direct reflection of this increase. On the other hand, this was not the case observed with GS addition. Moreover, in contrast to HFCS, a positive correlation was observed between the GS% and CC% ($r=0.863$).

Glucose to water ratio (G/W) is an important parameter for honey crystallization due to lower solubility of glucose compared to fructose (Al-Habsi et al., 2013). Usually a level of 2.10 is considered as the limit for crystallization. With HFCS addition, due to higher water content G/W ratio decreased and a perfectly high correlation was detected between the G/W ratio and CC% values (Fig. 3.14).

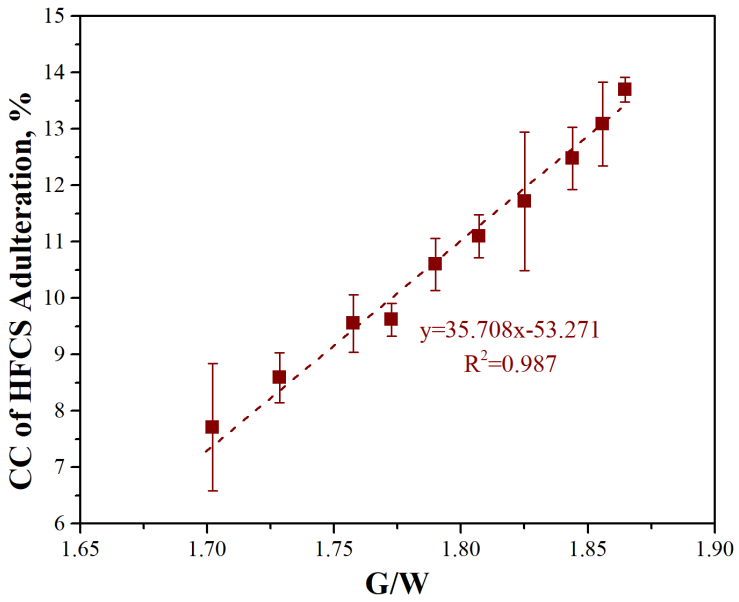

Figure 3.14. MSE solid component of HFCS adulteration with respect to glucose to water ratio

As stated before, GS addition did not change the water content very much. Although water activity and T_1 relaxations times increased with increasing GS%, there was a significant decrease on the T_2 values of the fast-relaxing component ($p<0.05$). T_2 values of this component and CC% were also highly correlated. As T_2 values decreased; CC% increased significantly ($r=-0.767$).

Brix values were 71.93, 82.50 and 82.93 for HFCS, GS and honey, respectively. HFCS included mostly glucose and fructose whereas GS had ~32% maltose and ~25% higher order sugars (>DP_3). Solubility of fructose and glucose are 79 and 47 g per 100 g solution, respectively at the measurement temperature (Alves et al., 2007; Crestani et al., 2013). On the other hand maltose has a solubility of 48 g per 100 g solution (Gong et al., 2012). Although visible crystals were not observed in the honey samples, solubility of maltose being lower than the monosaccharides was explained as the major reason for the increase in CC% values with GS addition. Higher order sugars could also have contributed to the increase in CC%. The observed decrease

on the relaxation times of the fast component was also an indication that more solids were being associated with that proton pool and confirmed the findings of the MSE experiments.

3.3 Melting Experiments

For the crystallized honey samples, the RF coil of the magnet was heated to 50°C, and the crystallized samples were monitored for melting. The result was a nice exponential decay, as seen in Fig. 3.15.

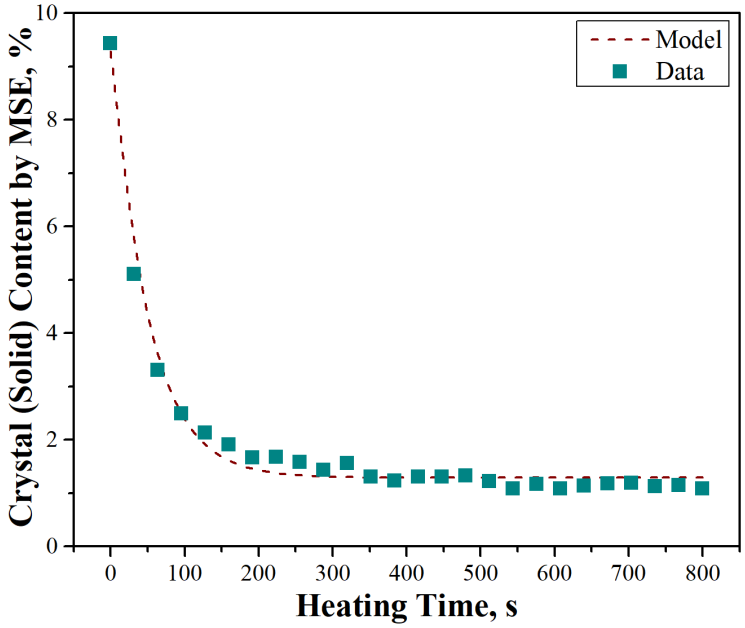

Figure 3.15. Crystallinity change during melting at 50°C

During measuring the melting behavior, the crystallized honey sample was heated from 14°C to 50°C for 800 seconds, and it was observed that 99.33% of the crystalline portion melted by 243rd seconds of thermal treatment. Thus, by using this information, it could be estimated that the time required for the crystal melting process at 50°C was 243 seconds for this honey.

If it is assumed that the thermal capacity of an NMR probe is much higher than the one of a sample, a cold sample at T_{sample} placed into NMR magnet at the temperature of T_{magnet} will be heated up without a noticeable influence on the magnet temperature. In such a case, the rate of heating dT_{sample}/dt will be proportional to the difference ($T_{sample} - T_{magnet}$) and obey the inversed exponential decay (initial and boundary conditions are $T_{sample}(0)$ and T_{magnet})

$$T_{sample}(t) = T_{sample}(0) + (T_{magnet} - T_{sample}(0))ae^{-t/t_{heating}} \textbf{ (Eqn. 3)}$$

It was empirically found that the behavior of the NMR value (Eqn. 4) during the heating process could also well be fitted with an exponent;

$$Cr = 7.99e^{-t/48.591} + 1.292 \textbf{ (Eqn. 4)}$$

with characteristic time τ = 48.591. Knowing that at 5*τ a simple exponential decay loses 99.33% of its initial value, we suggest using 5*τ (in this case ~243 seconds) for the removal of most of the crystals in this honey. This '*time'* information could be valuable for processes like pasteurization or RF heating, which can be applied to honey samples.

CHAPTER 4

CONCLUSION

TD-NMR is an easy to use analytical technique that can be performed on benchtop, low to medium field systems. Many characterization and quality control experiments could be conducted on food systems by using a single NMR equipment. Solid Fat Content (SFC) measurement has already been established as an official standard method for fat and chocolate industry. The method is based on measuring the crystal content of the samples with the simplest NMR sequence that is the Free Induction Decay.

In the first part of this study, this approach was used to monitor crystallization and melting kinetics on honey samples by utilizing the magic sandwich echo sequence. MSE is advantageous as it solves the problem of dead time (the time lost due to NMR hardware) and provides high signal to noise ratios. The results of this study showed that crystallization of glucose seeded honey followed a consistent kinetics relation complementary with DSC experiment results. Useful information about the state and behavior of crystallization was obtained by using the MSE sequence. Relaxation time measurements also confirmed the results.

In the second part of this study, adulterated honey samples were measured in terms of their relaxation times and solid contents by using TD-NMR. The results showed that it is possible to differentiate the unadulterated and adulterated honey samples by using TD-NMR relaxation times and MSE value. Higher maltose content of GS and changing glucose to water content of HFCS adulteration with MSE output resulted in higher correlation. Use of TD-NMR systems can be a good tool to detect adulteration.

In the last part of this study, melting experiments for crystallized honey were performed, and results showed that the melting behavior could be explained by a mono-exponential decay, and such an approach could be utilized for many other melting processes in the food industry.

REFERENCES

Acquarone, C., Buera, P., & Elizalde, B. (2007). Pattern of pH and electrical conductivity upon honey dilution as a complementary tool for discriminating geographical origin of honeys. *Food Chemistry*, *101*(2), 695–703. https://doi.org/10.1016/j.foodchem.2006.01.058

Al-Habsi, N. A., Davis, F. J., & Niranjan, K. (2013). Development of Novel Methods to Determine Crystalline Glucose Content of Honey Based on DSC, HPLC, and Viscosity Measurements, and Their Use to Examine the Setting Propensity of Honey. *Journal of Food Science*, *78*(6). https://doi.org/10.1111/1750-3841.12103

Alves, L. A., Almeida E Silva, J. B., & Giulietti, M. (2007). Solubility of D-glucose in water and ethanol/water mixtures. *Journal of Chemical and Engineering Data*, *52*(6), 2166–2170. https://doi.org/10.1021/je700177n

Amaral-Fonseca, M., Morellon-Sterling, R., Fernández-Lafuente, R., & Tardioli, P. W. (2020). Optimization of simultaneous saccharification and isomerization of dextrin to high fructose syrup using a mixture of immobilized amyloglucosidase and glucose isomerase. *Catalysis Today*, *March*, 0–1. https://doi.org/10.1016/j.cattod.2020.03.021

Anklam, E. (1998). A review of the analytical methods to determine the geographical and botanical origin of honey. *Food Chemistry*, *63*(4), 549–562. https://doi.org/10.1016/S0308-8146(98)00057-0

AOCS Official Method Cd 16b-93. (2009a). Solid fat content (SFC) by low-resolution nuclear magnetic resonance - the direct method. In *Official Methods and Recommended Practices of the AOCS*. https://doi.org/10.1111/j.1750-3841.2011.02241.x

AOCS Official Method Cd 16b-93. (2009b). Solid fat content (SFC) by low-resolution nuclear magnetic resonance - the direct method. In *Official Methods and Recommended Practices of the AOCS*. https://doi.org/10.1111/j.1750-3841.2011.02241.x

Bakier, S. (2017). Rheological Properties of Honey Honey in a Liquid and Crystallized State Crystallized State. *Honey Analysis*. https://doi.org/10.5772/67035

Bakier, S., Miastkowski, K., & Bakoniuk, J. R. (2016). Rheological properties of some honeys in liquefied and crystallised states. *Journal of Apicultural Science*, *60*(2), 153–166. https://doi.org/10.1515/JAS-2016-0026

Batt, P. J., & Liu, A. (2012). Consumer behaviour towards honey products in Western Australia. *British Food Journal*, *114*(2), 285–297. https://doi.org/10.1108/00070701211202449

Belay, A., Solomon, W. K., Bultossa, G., Adgaba, N., & Melaku, S. (2015). Botanical origin, colour, granulation, and sensory properties of the Harenna forest honey, Bale, Ethiopia. *Food Chemistry*, *167*, 213–219. https://doi.org/https://doi.org/10.1016/j.foodchem.2014.06.080

Belitz, H. D., Burghagen, M., Grosch, W., & Schieberle, P. (2004). *Food Chemistry*. Springer Berlin Heidelberg. https://books.google.com.tr/books?id=_QWbLTSL6HoC

Bentivenga, G., D'Auria, M., Fedeli, P., Mauriello, G., & Racioppi, R. (2004). SPME-GC-MS analysis of volatile organic compounds in honey from Basilicata. Evidence for the presence of pollutants from anthropogenic activities. *International Journal of Food Science and Technology*, *39*(10), 1079–1086. https://doi.org/10.1111/j.1365-2621.2004.00889.x

Boukraâ, L. (2013). *Honey in Traditional and Modern Medicine*. CRC Press. https://books.google.com.tr/books?id=OabMBQAAQBAJ

Brunauer, S., Emmett, P. H., & Teller, E. (1938). Adsorption of Gases in Multimolecular Layers. *Journal of the American Chemical Society*, *60*(2), 309–319. https://doi.org/10.1021/ja01269a023

Burucu, V. (2017). *Arıcılık*. TEPGE. https://arastirma.tarimorman.gov.tr/tepge/Belgeler/PDF Ürün Raporları/2017 Ürün Raporları/Arıcılık Ürün Raporu 2017-295.pdf

Carter, P., Gray, L. J., Talbot, D., Morris, D. H., Khunti, K., & Davies, M. J. (2013). Fruit and vegetable intake and the association with glucose parameters: A cross-sectional analysis of the Let's Prevent Diabetes Study. *European Journal of Clinical Nutrition*, *67*(1), 12–17. https://doi.org/10.1038/ejcn.2012.174

Caurie, M. (2011). Bound water: Its definition, estimation and characteristics. *International Journal of Food Science and Technology*, *46*(5), 930–934. https://doi.org/10.1111/j.1365-2621.2011.02581.x

Chiu, M. H., & Prenner, E. J. (2011). Differential scanning calorimetry: An invaluable tool for a detailed thermodynamic characterization of macromolecules and their interactions. *Journal of Pharmacy & Bioallied Sciences*, *3*(1), 39–59. https://doi.org/10.4103/0975-7406.76463

Çinar, S. B., Ekşi, A., & Coşkun, I. (2014). Carbon isotope ratio (13C/12C) of pine honey and detection of HFCS adulteration. *Food Chemistry*, *157*, 10–13. https://doi.org/10.1016/j.foodchem.2014.02.006

Codex Alimentarius Commission. (2001a). Codex Alimentarius Commission Standards. *Codex Stan 12-1981*.

Codex Alimentarius Commission. (2001b). Codex Standard for Honey, CODEX STAN 12-1981. *Codex Alimentarius Commission FAO/OMS*, 1–8.

Cosmina, M., Gallenti, G., Marangon, F., & Troiano, S. (2016). Attitudes towards honey among Italian consumers: A choice experiment approach. *Appetite*, *99*, 52–58. https://doi.org/10.1016/j.appet.2015.12.018

Crane, E. (1999). *The World History of Beekeeping and Honey Hunting*. Routledge. https://books.google.com.tr/books?id=ANTSvKj1AZEC

Crane, Eva. (1975). *Honey: A Comprehensive Survey*. Bee Research Association. https://books.google.com.tr/books?id=rdg4AQAAIAAJ

Crane, Eva. (1991). Honey from honeybees and other insects. *Ethology Ecology and Evolution*, *3*(June), 100–105. https://doi.org/10.1080/03949370.1991.10721919

Crestani, C. E., Bernardo, A., Costa, C. B. B., & Giulietti, M. (2013). Fructose solubility in mixed (ethanol + water) solvent: Experimental data and comparison among different thermodynamic models. *Journal of Chemical and Engineering Data*, *58*(11), 3039–3045. https://doi.org/10.1021/je400471m

Crestani, C. E., Bernardo, A., Costa, C. B. B., & Giulietti, M. (2018). Experimental data and estimation of sucrose solubility in impure solutions. *Journal of Food Engineering*, *218*, 14–23. https://doi.org/10.1016/j.jfoodeng.2017.08.023

Cui, Z. W., Sun, L. J., Chen, W., & Sun, D. W. (2008). Preparation of dry honey by microwave-vacuum drying. *Journal of Food Engineering*, *84*(4), 582–590. https://doi.org/10.1016/j.jfoodeng.2007.06.027

de-Miguel, S., Pukkala, T., & Yeşil, A. (2014). Integrating pine honeydew honey production into forest management optimization. *European Journal of Forest Research*, *133*(3), 423–432. https://doi.org/10.1007/s10342-013-0774-2

Dejong, A. E., & Hartel, R. W. (2016). Determination of sorbitol crystal content and crystallization rate using TD-NMR. *Journal of Food Engineering*, *178*, 117–123. https://doi.org/10.1016/j.jfoodeng.2016.01.012

Dyce, E. J. (1975). Producing finely granulated or creamed honey. In *Honey: A Comprehensive Survey. E. Crane, ed: Vol. v. 1975*.

Escriche, I., Kadar, M., Domenech, E., & Gil-Sánchez, L. (2012). A potentiometric electronic tongue for the discrimination of honey according to the botanical origin. Comparison with traditional methodologies: Physicochemical parameters and volatile profile. *Journal of Food Engineering*, *109*(3), 449–456. https://doi.org/https://doi.org/10.1016/j.jfoodeng.2011.10.036

Escriche, I., Tanleque-Alberto, F., Visquert, M., & Oroian, M. (2017). Physicochemical and rheological characterization of honey from Mozambique. *LWT*, *86*, 108–115. https://doi.org/https://doi.org/10.1016/j.lwt.2017.07.053

Escuredo, O., Rodríguez-Flores, M. S., Rojo-Martínez, S., & Seijo, M. C. (2019). Contribution to the chromatic characterization of unifloral honeys from Galicia (NW Spain). *Foods*, *8*(7), 10–13. https://doi.org/10.3390/foods8070233

Fechner, D. C., Hidalgo, M. J., Ruiz Díaz, J. D., Gil, R. A., & Pellerano, R. G. (2020). Geographical origin authentication of honey produced in Argentina. *Food Bioscience*, *33*, 100483. https://doi.org/https://doi.org/10.1016/j.fbio.2019.100483

Gallardo-Velázquez, T., Osorio-Revilla, G., Loa, M. Z. de, & Rivera-Espinoza, Y. (2009). Application of FTIR-HATR spectroscopy and multivariate analysis to the quantification of adulterants in Mexican honeys. *Food Research International*, *42*(3), 313–318. https://doi.org/10.1016/j.foodres.2008.11.010

Gill, R. S., Hans, V. S., Singh, S., Pal Singh, P., & Dhaliwal, S. S. (2015). A small scale honey dehydrator. *Journal of Food Science and Technology*, *52*(10), 6695–6702. https://doi.org/10.1007/s13197-015-1760-0

Giraudon, S., Danzart, M., & Merle, M. H. (2000). Deuterium nuclear magnetic resonance spectroscopy and stable carbon isotope ratio analysis/mass spectrometry of certain monofloral honeys. *Journal of AOAC International*, *83*(6), 1401–1409.

Gleiter, R. A., Horn, H., & Isengard, H. D. (2006). Influence of type and state of crystallisation on the water activity of honey. *Food Chemistry*, *96*(3), 441–445. https://doi.org/10.1016/j.foodchem.2005.03.051

Gómez-díaz, D., Navaza, J. M., Quintáns-riveiro, L. C., Gómez-díaz, D., & Navaza, J. M. (2009). *Effect of Temperature on the Viscosity of Honey*. *2912*. https://doi.org/10.1080/10942910701813925

Gong, X., Wang, C., Zhang, L., & Qu, H. (2012). Solubility of xylose, mannose, maltose monohydrate, and trehalose dihydrate in ethanol-water solutions. *Journal of Chemical and Engineering Data*, *57*(11), 3264–3269. https://doi.org/10.1021/je300885g

Gounari, S. (2006). Studies on the phenology of marchalina hellenica (gen.) (hemiptera: Coccoidea, margarodidae) in relation to honeydew flow. *Journal of Apicultural Research*, *45*(1), 8–12. https://doi.org/10.1080/00218839.2006.11101305

Grunin, L., Oztop, M. H., Guner, S., & Baltaci, S. F. (2019). Exploring the crystallinity of different powder sugars through solid echo and magic sandwich echo sequences. *Magnetic Resonance in Chemistry*, *March*, 607–615. https://doi.org/10.1002/mrc.4866

Hornsey, I. (2003). *A History of Beer and Brewing* (1st ed.). The Royal Society of Chemistry.

International Honey Commission (ICH). (2009). Harmonised Methods of the International Honey Commission. *Bee Product Science*, 1–63. https://doi.org/10.1007/s13398-014-0173-7.2

Jelesarov, I., & Bosshard, H. R. (1999). Isothermal titration calorimetry and differential scanning calorimetry as complementary tools to investigate the energetics of biomolecular recognition. *Journal of Molecular Recognition : JMR*, *12*(1), 3–18. https://doi.org/10.1002/(SICI)1099-1352(199901/02)12:1<3::AID-JMR441>3.0.CO;2-6

Keim, N. L., Stanhope, K. L., & Havel, P. J. (2015). Fructose and High-Fructose Corn Syrup. In *Encyclopedia of Food and Health* (1st ed.). Elsevier Ltd. https://doi.org/10.1016/B978-0-12-384947-2.00333-0

Kirtil, E., & Oztop, M. H. (2016). 1H Nuclear Magnetic Resonance Relaxometry and Magnetic Resonance Imaging and Applications in Food Science and Processing. *Food Engineering Reviews*, *8*(1), 1–22. https://doi.org/10.1007/s12393-015-9118-y

Kruk, D., Herrmann, A., & Rössler, E. A. (2012). Field-cycling NMR relaxometry of viscous liquids and polymers. *Progress in Nuclear Magnetic Resonance Spectroscopy*, *63*, 33–64. https://doi.org/10.1016/j.pnmrs.2011.08.001

Laos, K., Kirs, E., Pall, R., & Martverk, K. (2011). The crystallization behaviour of Estonian honeys. *Agronomy Research*, *9*(SPPL. ISS. 2), 427–432.

Le Botlan, D., Casseron, F., & Lantier, F. (1998). Polymorphism of sugars studied by time domain NMR. *Analusis*, *26*(5), 198–204. https://doi.org/10.1051/analusis:1998135

Lupano, C. E. (1997). DSC study of honey granulation stored at various temperatures. *Food Research International*, *30*(9), 683–688. https://doi.org/10.1016/S0963-9969(98)00030-1

Ma, M., Wang, Y., Wang, M., Jane, J. lin, & Du, S. kui. (2017). Physicochemical properties and in vitro digestibility of legume starches. *Food Hydrocolloids*, *63*, 249–255. https://doi.org/10.1016/j.foodhyd.2016.09.004

Marchese, C. M. (2009). *Honeybee: Lessons from an Accidental Beekeeper*. Black Dog & Leventhal Publishers, Incorporated. https://books.google.com.tr/books?id=WlATdvevk14C

Maus, A., Hertlein, C., & Saalwächter, K. (2006). A robust proton NMR method to investigate hard/soft ratios, crystallinity, and component mobility in polymers. *Macromolecular Chemistry and Physics*, *207*(13), 1150–1158. https://doi.org/10.1002/macp.200600169

McGee, H. (1984). On food and cooking: the scinece and the lore of the kitchen. In *New York, Scribner*.

Mesías, M., Sáez-Escudero, L., Morales, F. J., & Delgado-Andrade, C. (2019). Reassessment of acrylamide content in breakfast cereals. Evolution of the Spanish market from 2006 to 2018. *Food Control*, *105*(May), 94–101. https://doi.org/10.1016/j.foodcont.2019.05.026

Moreira, R. F. A., Trugo, L. C., Pietroluongo, M., & De Maria, C. A. B. (2002). Flavor composition of cashew (Anacardium occidentale) and marmeleiro (Croton species) honeys. *Journal of Agricultural and Food Chemistry*, *50*(26), 7616–7621. https://doi.org/10.1021/jf020464b

Namlı, S. (2019). *Microwave glycation of soy protein isolate* (Issue August) [Middle East Technical University]. http://etd.lib.metu.edu.tr/upload/12623713/index.pdf

Papon, A., Saalwächter, K., Schäler, K., Guy, L., Lequeux, F., & Montes, H. (2011). Low-Field NMR Investigations of Nanocomposites: Polymer Dynamics and Network Effects. *Macromolecules*, *44*(4), 913–922. https://doi.org/10.1021/ma102486x

Petracci, M., Laghi, L., Rimini, S., Rocculi, P., Capozzi, F., & Cavani, C. (2014). Chicken breast meat marinated with increasing levels of sodium bicarbonate. *Journal of Poultry Science*. https://doi.org/10.2141/jpsa.0130079

Pieruccini, M., Sturniolo, S., Corti, M., & Rigamonti, A. (2015). A novel analysis for the NMR magic sandwich echo in polymers: application to the α-relaxation in polybutadiene. *The European Physical Journal B*, *88*(11), 283. https://doi.org/10.1140/epjb/e2015-60417-6

Płowaś-Korus, I., Masewicz, Ł., Szwengiel, A., Rachocki, A., Baranowska, H. M., & Medycki, W. (2018). A novel method of recognizing liquefied honey. *Food Chemistry*, *245*(July 2017), 885–889. https://doi.org/10.1016/j.foodchem.2017.11.087

Popek, S. (2002). A procedure to identify a honey type. *Food Chemistry*, *79*(3), 401–406. https://doi.org/10.1016/S0308-8146(02)00391-6

Porter, T., & Hartel, R. W. (2013). Quantifying Sucrose Crystal Content in Fondant. *The Manufacturing Confectioner*, *January*, 61–64.

Ribeiro, R. D. O. R., Máralém, E. T., Carneiro, C. D. S., Monteiro, M. L. G., Júnior, C. C., & Jesus, E. F. O. De. (2014). Detection of honey adulteration of high fructose corn syrup by Low Field Nuclear Magnetic Resonance (LF 1H NMR). *Journal of Food Engineering*, *135*, 39–43. https://doi.org/10.1016/j.jfoodeng.2014.03.009

Ribeiro, R. de O. R., Mársico, E. T., Carneiro, C. da S., Monteiro, M. L. G., Conte Júnior, C. A., Mano, S., & de Jesus, E. F. O. (2014). Classification of Brazilian honeys by physical and chemical analytical methods and low field nuclear magnetic resonance (LF 1H NMR). *LWT - Food Science and Technology*, *55*(1), 90–95. https://doi.org/10.1016/j.lwt.2013.08.004

Root, A. I., & Root, E. R. (1919). *The A B C and X Y Z of bee culture: a cyclopedia of everything pertaining to the care of the honeybee; bees, hives, honey, implements, honey plants, etc. Facts gleaned from the experience of thousands of beekeepers and verified in the authors' apiary*. The A. R. Root company. https://books.google.com.tr/books?id=290cAQAAMAAJ

Rybak-Chmielewska, H., & Szczesna Pulawy (Poland). Apiculture Division), T. (Research I. of P. and F. (1999). Viscosity of honey. In *Pszczelnicze Zeszyty Naukowe (Poland): Vol. v. 43*.

Şahin, S., Şumnu, S. G., Hamamcı, H., İşçi, A., & Şakıyan, Ö. (2016). *Fluid Flow, Heat & Mass Transfer in Food Systems* (1st ed.). Nobel Yayıcılık.

Se, K. W., Wahab, R. A., Syed Yaacob, S. N., & Ghoshal, S. K. (2019). Detection techniques for adulterants in honey: Challenges and recent trends. *Journal of Food Composition and Analysis*, *80*(September 2018), 16–32. https://doi.org/10.1016/j.jfca.2019.04.001

Šedík, P., Horská, E., Skowron-Grabowska, B., & Illés, C. B. (2018). Generation marketing in strategic marketing management: Case study of honey market. *Polish Journal of Management Studies*, *18*(1), 326–337. https://doi.org/10.17512/pjms.2018.18.1.24

Sereia, M. J., Março, P. H., Perdoncini, M. R. G., Parpinelli, R. S., de Lima, E. G., & Anjo, F. A. (2017). Techniques for the Evaluation of Physicochemical Quality and Bioactive Compounds in Honey. In *Honey Analysis*. https://doi.org/10.5772/66839

Serra Bonvehi, J., Ventura Coll, F., & Orantes Bermejo, J. F. (2019). Characterization of avocado honey (Persea americana Mill.) produced in Southern Spain. *Food Chemistry*, *287*, 214–221. https://doi.org/https://doi.org/10.1016/j.foodchem.2019.02.068

Solomons, T. W. G., Fryhle, C. B., & Snyder, S. A. (2016). *Organic Chemistry*. Wiley. https://books.google.com.tr/books?id=hWLpCgAAQBAJ

Sturniolo, S., & Saalwächter, K. (2011). Breakdown in the efficiency factor of the mixed Magic Sandwich Echo: A novel NMR probe for slow motions. *Chemical Physics Letters*, *516*(1), 106–110. https://doi.org/https://doi.org/10.1016/j.cplett.2011.09.059

Subramanian, R., Umesh Hebbar, H., & Rastogi, N. K. (2007). Processing of Honey: A Review. *International Journal of Food Properties*, *10*(1), 127–143. https://doi.org/10.1080/10942910600981708

Tappi, S., Laghi, L., Dettori, A., Piana, L., Ragni, L., & Rocculi, P. (2019). Investigation of water state during induced crystallization of honey. *Food Chemistry*, *294*(April), 260–266. https://doi.org/10.1016/j.foodchem.2019.05.047

Terrab, A., González, A. G., Díez, M. J., & Heredia, F. J. (2003). Mineral content and electrical conductivity of the honeys produced in Northwest Morocco and their contribution to the characterisation of unifloral honeys. *Journal of the Science of Food and Agriculture*, *83*(7), 637–643. https://doi.org/10.1002/jsfa.1341

Tuberoso, C. I. G., Jerković, I., Sarais, G., Congiu, F., Marijanović, Z., & Kuś, P. M. (2014). Color evaluation of seventeen European unifloral honey types by means of spectrophotometrically determined CIE L â - Cab â - Hab ẫ chromaticity coordinates. *Food Chemistry*, *145*, 284–291. https://doi.org/10.1016/j.foodchem.2013.08.032

Vorwohl, G. (1964). Die beziehungen zwischen der elektrischen leitfähigkeit derhonige und ihrer trachtmässigen herkunft. *Les Annales de l'Abeille*, *7*(4), 301–309.

Wang, Q., Zhao, H., Zhu, M., Zhang, J., Cheng, N., & Cao, W. (2020). Method for identifying acacia honey adulterated by resin absorption: HPLC-ECD coupled with chemometrics. *Lwt*, *118*(November 2019), 108863. https://doi.org/10.1016/j.lwt.2019.108863

Wilkins, A. L., & Lu, Y. (1995). Extractives from New Zealand Honeys. 5. Aliphatic Dicarboxylic Acids in New Zealand Rewarewa (Knightea excelsa) Honey. *Journal of Agricultural and Food Chemistry*, *43*(12), 3021–3025. https://doi.org/10.1021/jf00060a006

Yadata, D. (2014). Detection of the Electrical Conductivity and Acidity of Honey from Different Areas of Tepi. *Food Science and Technology*, *2*(5), 59–63. https://doi.org/10.13189/fst.2014.020501

Yener, E., Ungan, S., & Özilgen, M. (1987). Drying Behavior of Honey-Starch Mixtures. *Journal of Food Science*, *52*(4), 1054–1058. https://doi.org/10.1111/j.1365-2621.1987.tb14274.x

Yilmaz, M. T., Tatlisu, N. B., Toker, O. S., Karaman, S., Dertli, E., Sagdic, O., & Arici, M. (2014). Steady, dynamic and creep rheological analysis as a novel approach to detect honey adulteration by fructose and saccharose syrups: Correlations with HPLC-RID results. *Food Research International*, *64*, 634–646. https://doi.org/10.1016/j.foodres.2014.07.009

Zamora, M. C., & Chirife, J. (2006). Determination of water activity change due to crystallization in honeys from Argentina. *Food Control*, *17*(1), 59–64. https://doi.org/10.1016/j.foodcont.2004.09.003

APPENDICES

A. Statistical Analyses for Crystallization Kinetics

Table 4.1 Pearson Correlation analysis for all factors of crystallization kinetics experiment

Correlation: Time, h; Crystal (Solid) Content, %; Melting Enthalpy, J/g; T22, ms; T21, ms; A22, %; A21, %; T1, ms

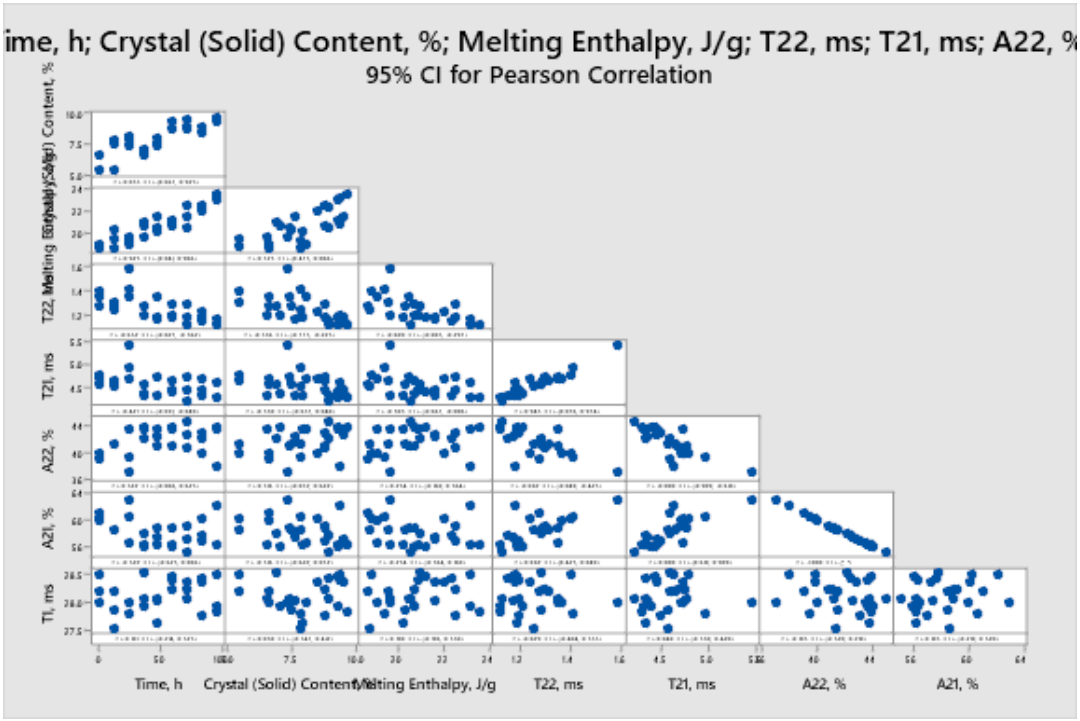

Method

Correlation type	Pearson
Rows used	27

ρ: pairwise Pearson correlation

Correlations

	Time, h	Crystal (Solid) Content, %	Melting Enthalpy, J/g	T22, ms	T21, ms	A22, %	A21, %
Crystal (Solid) Content, %	0.835						
Melting Enthalpy, J/g	0.925	0.725					
T22, ms	-0.652	-0.556	-0.609				
T21, ms	-0.421	-0.338	-0.385	0.943			
A22, %	0.322	0.316	0.234	-0.692	-0.808		
A21, %	-0.322	-0.316	-0.234	0.692	0.808	-1.000	
T1, ms	0.181	0.038	0.198	-0.029	0.048	-0.185	0.185

Pairwise Pearson Correlations

Sample 1	Sample 2	Correlation	95% CI for ρ	P-Value
Crystal (Solid) Content, %	Time, h	0.835	(0.667; 0.923)	0.000
Melting Enthalpy, J/g	Time, h	0.925	(0.841; 0.966)	0.000
T22, ms	Time, h	-0.652	(-0.827; -0.362)	0.000
T21, ms	Time, h	-0.421	(-0.691; -0.049)	0.029
A22, %	Time, h	0.322	(-0.066; 0.625)	0.102
A21, %	Time, h	-0.322	(-0.625; 0.066)	0.102
T1, ms	Time, h	0.181	(-0.214; 0.525)	0.366
Melting Enthalpy, J/g	Crystal (Solid) Content, %	0.725	(0.475; 0.866)	0.000
T22, ms	Crystal (Solid) Content, %	-0.556	(-0.773; -0.223)	0.003
T21, ms	Crystal (Solid) Content, %	-0.338	(-0.637; 0.048)	0.084
A22, %	Crystal (Solid) Content, %	0.316	(-0.072; 0.622)	0.108
A21, %	Crystal (Solid) Content, %	-0.316	(-0.622; 0.072)	0.108
T1, ms	Crystal (Solid) Content, %	0.038	(-0.347; 0.412)	0.852
T22, ms	Melting Enthalpy, J/g	-0.609	(-0.803; -0.297)	0.001
T21, ms	Melting Enthalpy, J/g	-0.385	(-0.667; -0.006)	0.048
A22, %	Melting Enthalpy, J/g	0.234	(-0.160; 0.564)	0.239
A21, %	Melting Enthalpy, J/g	-0.234	(-0.564; 0.160)	0.239
T1, ms	Melting Enthalpy, J/g	0.198	(-0.196; 0.538)	0.321
T21, ms	T22, ms	0.943	(0.876; 0.974)	0.000
A22, %	T22, ms	-0.692	(-0.849; -0.423)	0.000
A21, %	T22, ms	0.692	(0.423; 0.849)	0.000
T1, ms	T22, ms	-0.029	(-0.404; 0.355)	0.888
A22, %	T21, ms	-0.808	(-0.909; -0.618)	0.000
A21, %	T21, ms	0.808	(0.618; 0.909)	0.000
T1, ms	T21, ms	0.048	(-0.338; 0.420)	0.813
A21, %	A22, %	-1.000	(*; *)	*
T1, ms	A22, %	-0.185	(-0.528; 0.210)	0.356
T1, ms	A21, %	0.185	(-0.210; 0.528)	0.356

B. Statistical Analyses for Adulteration Determination

Table 4.2 ANOVA and Tukey's Comparison Test with 95% confidence level for determination of HFCS adulteration

General Linear Model: T22, ms versus HFCS, %

Method

Factor coding (-1; 0; +1)

Factor Information

Factor	Type	Levels	Values
HFCS, %	Fixed	11	0.00; 2.12; 5.13; 10.01; 14.95; 19.91; 25.14; 29.97; 39.93; 49.82; 100.00

Analysis of Variance

Source	DF	Adj SS	Adj MS	F-Value	P-Value
HFCS, %	10	1204.41	120.441	1000.60	0.000
Error	22	2.65	0.120		
Total	32	1207.06			

Model Summary

S	R-sq	R-sq(adj)	R-sq(pred)
0.346943	99.78%	99.68%	99.51%

Comparisons for T22, ms

Tukey Pairwise Comparisons: HFCS, %

Grouping Information Using the Tukey Method and 95% Confidence

HFCS, %	N	Mean	Grouping				
100.00	3	22.4533	A				
49.82	3	9.3367		B			
39.93	3	5.5540			C		
29.97	3	3.9900				D	
25.14	3	3.2420				D	E
19.91	3	2.7187					E
14.95	3	1.6867					F
10.01	3	1.4937					F
5.13	3	1.1813					F
2.12	3	1.1587					F
0.00	3	1.0076					F

Means that do not share a letter are significantly different.

General Linear Model: A22, % versus HFCS, %

Method

Factor coding (-1; 0; +1)

Factor Information

Factor	Type	Levels	Values
HFCS, %	Fixed	11	0.00; 2.12; 5.13; 10.01; 14.95; 19.91; 25.14; 29.97; 39.93; 49.82; 100.00

Analysis of Variance

Source	DF	Adj SS	Adj MS	F-Value	P-Value
HFCS, %	10	2810.00	281.000	75.76	0.000
Error	22	81.60	3.709		
Total	32	2891.60			

Model Summary

S	R-sq	R-sq(adj)	R-sq(pred)
1.92595	97.18%	95.90%	93.65%

Comparisons for A22, %

Tukey Pairwise Comparisons: HFCS, %

Grouping Information Using the Tukey Method and 95% Confidence

HFCS, %	N	Mean	Grouping		
49.82	3	63.9387	A		
100.00	3	55.4314		B	
0.00	3	40.8385			C
39.93	3	40.2777			C
19.91	3	38.4739			C
2.12	3	38.3737			C
5.13	3	37.3398			C	D
29.97	3	35.5921			C	D
25.14	3	35.5657			C	D
10.01	3	35.3689			C	D
14.95	3	31.7876				D

Means that do not share a letter are significantly different.

General Linear Model: T21, % versus HFCS, %

Method

Factor coding (-1; 0; +1)

Factor Information

Factor	Type	Levels	Values
HFCS, %	Fixed	11	0.00; 2.12; 5.13; 10.01; 14.95; 19.91; 25.14; 29.97; 39.93; 49.82; 100.00

Analysis of Variance

Source	DF	Adj SS	Adj MS	F-Value	P-Value
HFCS, %	10	10636.1	1063.61	76.18	0.000
Error	22	307.1	13.96		
Total	32	10943.2			

Model Summary

S	R-sq	R-sq(adj)	R-sq(pred)
3.73645	97.19%	95.92%	93.68%

Comparisons for T21, ms

Tukey Pairwise Comparisons: HFCS, %

Grouping Information Using the Tukey Method and 95% Confidence

HFCS, %	N	Mean	Grouping		
100.00	3	65.0367	A		
49.82	3	36.3767		B	
39.93	3	15.9500			C
29.97	3	11.8033			C D
25.14	3	9.9490			C D
19.91	3	8.6507			C D
14.95	3	6.1033			C D
10.01	3	5.3907			C D
5.13	3	4.5790			D
2.12	3	4.4270			D
0.00	3	4.0127			D

Means that do not share a letter are significantly different.

General Linear Model: A21, % versus HFCS, %

Method

Factor coding (-1; 0; +1)

Factor Information

Factor	Type	Levels	Values
HFCS, %	Fixed	11	0.00; 2.12; 5.13; 10.01; 14.95; 19.91; 25.14; 29.97; 39.93; 49.82; 100.00

Analysis of Variance

Source	DF	Adj SS	Adj MS	F-Value	P-Value
HFCS, %	10	2810.00	281.000	75.76	0.000
Error	22	81.60	3.709		
Total	32	2891.60			

Model Summary

S	R-sq	R-sq(adj)	R-sq(pred)
1.92595	97.18%	95.90%	93.65%

Comparisons for A21, %

Tukey Pairwise Comparisons: HFCS, %

Grouping Information Using the Tukey Method and 95% Confidence

HFCS, %	N	Mean	Grouping			
14.95	3	68.2124	A			
10.01	3	64.6311	A	B		
25.14	3	64.4343	A	B		
29.97	3	64.4079	A	B		
5.13	3	62.6602	A	B		
2.12	3	61.6263		B		
19.91	3	61.5261		B		
39.93	3	59.7223		B		
0.00	3	59.1615		B		
100.00	3	44.5686			C	
49.82	3	36.0613				D

Means that do not share a letter are significantly different.

General Linear Model: T2, ms versus HFCS, %

Method

Factor coding (-1; 0; +1)

Factor Information

Factor	Type	Levels	Values
HFCS, %	Fixed	11	0.00; 2.12; 5.13; 10.01; 14.95; 19.91; 25.14; 29.97; 39.93; 49.82; 100.00

Analysis of Variance

Source	DF	Adj SS	Adj MS	F-Value	P-Value
HFCS, %	10	2869.72	286.972	2821.42	0.000
Error	22	2.24	0.102		
Total	32	2871.96			

Model Summary

S	R-sq	R-sq(adj)	R-sq(pred)
0.318923	99.92%	99.89%	99.82%

Comparisons for T2, ms

Tukey Pairwise Comparisons: HFCS, %

Grouping Information Using the Tukey Method and 95% Confidence

HFCS, %	N	Mean	Grouping								
100.00	3	36.9220	A								
49.82	3	13.3377		B							
39.93	3	10.2196			C						
29.97	3	8.4641				D					
25.14	3	7.3737					E				
19.91	3	6.3980						F			
14.95	3	4.4592							G		
10.01	3	3.9076							G	H	
5.13	3	3.3947								H	I
2.12	3	3.2701								H	I
0.00	3	2.9673									I

Means that do not share a letter are significantly different.

General Linear Model: T1, ms versus HFCS, %

Method

Factor coding (-1; 0; +1)

Factor Information

Factor	Type	Levels	Values
HFCS, %	Fixed	11	0.00; 2.12; 5.13; 10.01; 14.95; 19.91; 25.14; 29.97; 39.93; 49.82; 100.00

Analysis of Variance

Source	DF	Adj SS	Adj MS	F-Value	P-Value
HFCS, %	10	798.843	79.8843	525.87	0.000
Error	22	3.342	0.1519		
Total	32	802.185			

Model Summary

S	R-sq	R-sq(adj)	R-sq(pred)
0.389755	99.58%	99.39%	99.06%

Comparisons for T1, ms

Tukey Pairwise Comparisons: HFCS, %

Grouping Information Using the Tukey Method and 95% Confidence

HFCS, %	N	Mean	Grouping		
100.00	3	45.5002	A		
49.82	3	29.9664		B	
0.00	3	28.8731		B	C
2.12	3	28.8688		B	C
5.13	3	28.7089			C
39.93	3	28.4396			C
10.01	3	28.4113			C
29.97	3	28.0213			C
25.14	3	27.9817			C
14.95	3	27.9807			C
19.91	3	27.8069			C

Means that do not share a letter are significantly different.

General Linear Model: Crystal (Solid) Component, % versus HFCS, %

Method

Factor coding (-1; 0; +1)

Factor Information

Factor	Type	Levels	Values
HFCS, %	Fixed	11	0.00; 2.12; 5.13; 10.01; 14.95; 19.91; 25.14; 29.97; 39.93; 49.82; 100.00

Analysis of Variance

Source	DF	Adj SS	Adj MS	F-Value	P-Value
HFCS, %	10	139.884	13.9884	31.91	0.000
Error	22	9.643	0.4383		
Total	32	149.527			

Model Summary

S	R-sq	R-sq(adj)	R-sq(pred)
0.662057	93.55%	90.62%	85.49%

Comparisons for Crystal (Solid) Component, %

Tukey Pairwise Comparisons: HFCS, %

Grouping Information Using the Tukey Method and 95% Confidence

HFCS, %	N	Mean	Grouping				
0.00	3	13.7023	A				
2.12	3	13.0960	A	B			
5.13	3	12.4877	A	B	C		
10.01	3	11.7250		B	C		
14.95	3	11.1007			C	D	
19.91	3	10.6073			C	D	
25.14	3	9.6203				D	E
29.97	3	9.5597				D	E
39.93	3	8.5990					E F
49.82	3	7.7127					E F
100.00	3	7.2183					F

Means that do not share a letter are significantly different.

Table 4.3 Pearson Correlation analysis for all factors of HFCS adulteration determination

Correlation: HFCS, %; T22, ms; A22, %; T21, ms; A21, %; T2, ms; T1, ms; Crystal (Solid) Component, %; G/W Ratio; Water Activity (aw); Moisture Content, %; Total Soluble Solid, Brix; Glucose, g/100 g; Fructose, g/100 g; Maltose, g/100 g

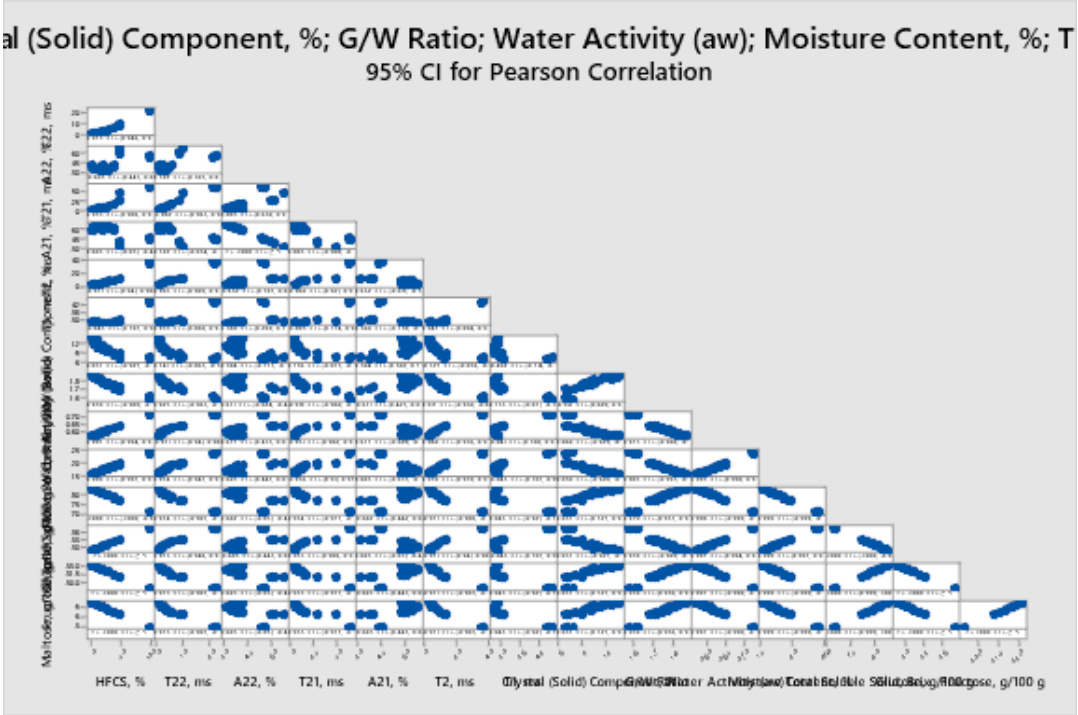

Method

Correlation type	Pearson
Rows used	33

ρ: pairwise Pearson correlation

Correlations

	HFCS, %	T22, ms	A22, %	T21, ms	A21, %	T2, ms	T1, ms
T22, ms	0.973						
A22, %	0.683	0.722					
T21, ms	0.953	0.982	0.805				
A21, %	-0.683	-0.722	-1.000	-0.805			
T2, ms	0.971	0.995	0.652	0.960	-0.652		
T1, ms	0.845	0.933	0.560	0.883	-0.560	0.947	
Crystal (Solid) Component, %	-0.857	-0.741	-0.584	-0.756	0.584	-0.727	-0.492
G/W Ratio	-0.978	-0.925	-0.671	-0.919	0.671	-0.917	-0.753
Water Activity (aw)	0.997	0.971	0.677	0.951	-0.677	0.968	0.841
Moisture Content, %	0.999	0.974	0.685	0.956	-0.685	0.970	0.845
Total Soluble Solid, Brix	-1.000	-0.974	-0.682	-0.954	0.682	-0.971	-0.845
Glucose, g/100 g	1.000	0.973	0.683	0.953	-0.683	0.971	0.845
Fructose, g/100 g	-1.000	-0.973	-0.683	-0.953	0.683	-0.971	-0.845
Maltose, g/100 g	-1.000	-0.973	-0.683	-0.953	0.683	-0.971	-0.845

	Crystal (Solid) Component, %	G/W Ratio	Water Activity (aw)	Moisture Content, %	Total Soluble Solid, Brix	Glucose, g/100 g
T22, ms						
A22, %						
T21, ms						
A21, %						
T2, ms						
T1, ms						
Crystal (Solid) Component, %						
G/W Ratio	0.912					
Water Activity (aw)	-0.860	-0.975				
Moisture Content, %	-0.858	-0.985	0.995			
Total Soluble Solid, Brix	0.857	0.979	-0.998	-0.999		
Glucose, g/100 g	-0.857	-0.978	0.997	0.999	-1.000	
Fructose, g/100 g	0.857	0.978	-0.997	-0.999	1.000	-1.000
Maltose, g/100 g	0.857	0.978	-0.997	-0.999	1.000	-1.000

	Fructose, g/100 g
T22, ms	
A22, %	
T21, ms	
A21, %	
T2, ms	
T1, ms	
Crystal (Solid) Component, %	
G/W Ratio	
Water Activity (aw)	
Moisture Content, %	
Total Soluble Solid, Brix	
Glucose, g/100 g	
Fructose, g/100 g	
Maltose, g/100 g	1.000

Pairwise Pearson Correlations

Sample 1	Sample 2	Correlation	95% CI for ρ	P-Value
T22, ms	HFCS, %	0.973	(0.946; 0.987)	0.000
A22, %	HFCS, %	0.683	(0.443; 0.831)	0.000
T21, ms	HFCS, %	0.953	(0.906; 0.977)	0.000
A21, %	HFCS, %	-0.683	(-0.831; -0.443)	0.000
T2, ms	HFCS, %	0.971	(0.941; 0.985)	0.000
T1, ms	HFCS, %	0.845	(0.707; 0.921)	0.000
Crystal (Solid) Component, %	HFCS, %	-0.857	(-0.927; -0.727)	0.000
G/W Ratio	HFCS, %	-0.978	(-0.989; -0.956)	0.000
Water Activity (aw)	HFCS, %	0.997	(0.994; 0.998)	0.000
Moisture Content, %	HFCS, %	0.999	(0.997; 0.999)	0.000
Total Soluble Solid, Brix	HFCS, %	-1.000	(-1.000; -0.999)	0.000
Glucose, g/100 g	HFCS, %	1.000	(*; *)	*
Fructose, g/100 g	HFCS, %	-1.000	(*; *)	*
Maltose, g/100 g	HFCS, %	-1.000	(*; *)	*
A22, %	T22, ms	0.722	(0.503; 0.854)	0.000
T21, ms	T22, ms	0.982	(0.963; 0.991)	0.000
A21, %	T22, ms	-0.722	(-0.854; -0.503)	0.000
T2, ms	T22, ms	0.995	(0.989; 0.997)	0.000
T1, ms	T22, ms	0.933	(0.868; 0.967)	0.000
Crystal (Solid) Component, %	T22, ms	-0.741	(-0.865; -0.534)	0.000
G/W Ratio	T22, ms	-0.925	(-0.963; -0.853)	0.000
Water Activity (aw)	T22, ms	0.971	(0.941; 0.986)	0.000
Moisture Content, %	T22, ms	0.974	(0.947; 0.987)	0.000
Total Soluble Solid, Brix	T22, ms	-0.974	(-0.987; -0.947)	0.000
Glucose, g/100 g	T22, ms	0.973	(0.946; 0.987)	0.000
Fructose, g/100 g	T22, ms	-0.973	(-0.987; -0.946)	0.000
Maltose, g/100 g	T22, ms	-0.973	(-0.987; -0.946)	0.000
T21, ms	A22, %	0.805	(0.638; 0.900)	0.000
A21, %	A22, %	-1.000	(*; *)	*
T2, ms	A22, %	0.652	(0.397; 0.813)	0.000
T1, ms	A22, %	0.560	(0.269; 0.758)	0.001
Crystal (Solid) Component, %	A22, %	-0.584	(-0.773; -0.302)	0.000
G/W Ratio	A22, %	-0.671	(-0.824; -0.425)	0.000
Water Activity (aw)	A22, %	0.677	(0.435; 0.828)	0.000
Moisture Content, %	A22, %	0.685	(0.447; 0.833)	0.000
Total Soluble Solid, Brix	A22, %	-0.682	(-0.831; -0.442)	0.000
Glucose, g/100 g	A22, %	0.683	(0.443; 0.831)	0.000
Fructose, g/100 g	A22, %	-0.683	(-0.831; -0.443)	0.000
Maltose, g/100 g	A22, %	-0.683	(-0.831; -0.443)	0.000
A21, %	T21, ms	-0.805	(-0.900; -0.638)	0.000
T2, ms	T21, ms	0.960	(0.921; 0.980)	0.000
T1, ms	T21, ms	0.883	(0.774; 0.941)	0.000
Crystal (Solid) Component, %	T21, ms	-0.756	(-0.873; -0.557)	0.000
G/W Ratio	T21, ms	-0.919	(-0.960; -0.841)	0.000
Water Activity (aw)	T21, ms	0.951	(0.902; 0.976)	0.000
Moisture Content, %	T21, ms	0.956	(0.911; 0.978)	0.000
Total Soluble Solid, Brix	T21, ms	-0.954	(-0.977; -0.908)	0.000
Glucose, g/100 g	T21, ms	0.953	(0.906; 0.977)	0.000
Fructose, g/100 g	T21, ms	-0.953	(-0.977; -0.906)	0.000
Maltose, g/100 g	T21, ms	-0.953	(-0.977; -0.906)	0.000
T2, ms	A21, %	-0.652	(-0.813; -0.397)	0.000
T1, ms	A21, %	-0.560	(-0.758; -0.269)	0.001
Crystal (Solid) Component, %	A21, %	0.584	(0.302; 0.773)	0.000
G/W Ratio	A21, %	0.671	(0.425; 0.824)	0.000

Water Activity (aw)	A21, %	-0.677	(-0.828; -0.435)	0.000
Moisture Content, %	A21, %	-0.685	(-0.833; -0.447)	0.000
Total Soluble Solid, Brix	A21, %	0.682	(0.442; 0.831)	0.000
Glucose, g/100 g	A21, %	-0.683	(-0.831; -0.443)	0.000
Fructose, g/100 g	A21, %	0.683	(0.443; 0.831)	0.000
Maltose, g/100 g	A21, %	0.683	(0.443; 0.831)	0.000
T1, ms	T2, ms	0.947	(0.894; 0.973)	0.000
Crystal (Solid) Component, %	T2, ms	-0.727	(-0.856; -0.511)	0.000
G/W Ratio	T2, ms	-0.917	(-0.958; -0.837)	0.000
Water Activity (aw)	T2, ms	0.968	(0.936; 0.984)	0.000
Moisture Content, %	T2, ms	0.970	(0.939; 0.985)	0.000
Total Soluble Solid, Brix	T2, ms	-0.971	(-0.986; -0.941)	0.000
Glucose, g/100 g	T2, ms	0.971	(0.941; 0.985)	0.000
Fructose, g/100 g	T2, ms	-0.971	(-0.985; -0.941)	0.000
Maltose, g/100 g	T2, ms	-0.971	(-0.985; -0.941)	0.000
Crystal (Solid) Component, %	T1, ms	-0.492	(-0.714; -0.178)	0.004
G/W Ratio	T1, ms	-0.753	(-0.871; -0.552)	0.000
Water Activity (aw)	T1, ms	0.841	(0.700; 0.919)	0.000
Moisture Content, %	T1, ms	0.845	(0.707; 0.921)	0.000
Total Soluble Solid, Brix	T1, ms	-0.845	(-0.921; -0.707)	0.000
Glucose, g/100 g	T1, ms	0.845	(0.707; 0.921)	0.000
Fructose, g/100 g	T1, ms	-0.845	(-0.921; -0.707)	0.000
Maltose, g/100 g	T1, ms	-0.845	(-0.921; -0.707)	0.000
G/W Ratio	Crystal (Solid) Component, %	0.912	(0.828; 0.956)	0.000
Water Activity (aw)	Crystal (Solid) Component, %	-0.860	(-0.929; -0.733)	0.000
Moisture Content, %	Crystal (Solid) Component, %	-0.858	(-0.928; -0.730)	0.000
Total Soluble Solid, Brix	Crystal (Solid) Component, %	0.857	(0.727; 0.927)	0.000
Glucose, g/100 g	Crystal (Solid) Component, %	-0.857	(-0.927; -0.727)	0.000
Fructose, g/100 g	Crystal (Solid) Component, %	0.857	(0.727; 0.927)	0.000
Maltose, g/100 g	Crystal (Solid) Component, %	0.857	(0.727; 0.927)	0.000
Water Activity (aw)	G/W Ratio	-0.975	(-0.988; -0.950)	0.000
Moisture Content, %	G/W Ratio	-0.985	(-0.993; -0.969)	0.000
Total Soluble Solid, Brix	G/W Ratio	0.979	(0.957; 0.990)	0.000
Glucose, g/100 g	G/W Ratio	-0.978	(-0.989; -0.956)	0.000
Fructose, g/100 g	G/W Ratio	0.978	(0.956; 0.989)	0.000
Maltose, g/100 g	G/W Ratio	0.978	(0.956; 0.989)	0.000
Moisture Content, %	Water Activity (aw)	0.995	(0.990; 0.998)	0.000
Total Soluble Solid, Brix	Water Activity (aw)	-0.998	(-0.999; -0.996)	0.000
Glucose, g/100 g	Water Activity (aw)	0.997	(0.994; 0.998)	0.000
Fructose, g/100 g	Water Activity (aw)	-0.997	(-0.998; -0.994)	0.000
Maltose, g/100 g	Water Activity (aw)	-0.997	(-0.998; -0.994)	0.000
Total Soluble Solid, Brix	Moisture Content, %	-0.999	(-0.999; -0.997)	0.000
Glucose, g/100 g	Moisture Content, %	0.999	(0.997; 0.999)	0.000
Fructose, g/100 g	Moisture Content, %	-0.999	(-0.999; -0.997)	0.000
Maltose, g/100 g	Moisture Content, %	-0.999	(-0.999; -0.997)	0.000
Glucose, g/100 g	Total Soluble Solid, Brix	-1.000	(-1.000; -0.999)	0.000
Fructose, g/100 g	Total Soluble Solid, Brix	1.000	(0.999; 1.000)	0.000
Maltose, g/100 g	Total Soluble Solid, Brix	1.000	(0.999; 1.000)	0.000
Fructose, g/100 g	Glucose, g/100 g	-1.000	(*; *)	*
Maltose, g/100 g	Glucose, g/100 g	-1.000	(*; *)	*
Maltose, g/100 g	Fructose, g/100 g	1.000	(*; *)	*

Table 4.4 ANOVA and Tukey's Comparison Test with 95% confidence level for determination of GS adulteration

General Linear Model: T22, ms versus GS, %

Method

Factor coding (-1; 0; +1)

Factor Information

Factor	Type	Levels	Values
GS, %	Fixed	11	0.00; 2.22; 5.05; 10.09; 14.98; 20.33; 25.42; 29.55; 39.82; 49.69; 100.00

Analysis of Variance

Source	DF	Adj SS	Adj MS	F-Value	P-Value
GS, %	10	0.94218	0.094218	36.05	0.000
Error	22	0.05749	0.002613		
Total	32	0.99967			

Model Summary

S	R-sq	R-sq(adj)	R-sq(pred)
0.0511200	94.25%	91.63%	87.06%

Comparisons for T22, ms

Tukey Pairwise Comparisons: GS, %

Grouping Information Using the Tukey Method and 95% Confidence

GS, %	N	Mean	Grouping		
2.22	3	1.02733	A		
0.00	3	1.00760	A		
5.05	3	0.97567	A		
10.09	3	0.88567	A	B	
14.98	3	0.81337		B	C
20.33	3	0.78363		B	C
25.42	3	0.76677		B	C
29.55	3	0.75443		B	C
39.82	3	0.69577			C
49.69	3	0.67403			C
100.00	3	0.41177			D

Means that do not share a letter are significantly different.

General Linear Model: A22, % versus GS, %

Method

Factor coding (-1; 0; +1)

Factor Information

Factor	Type	Levels	Values
GS, %	Fixed	11	0.00; 2.22; 5.05; 10.09; 14.98; 20.33; 25.42; 29.55; 39.82; 49.69; 100.00

Analysis of Variance

Source	DF	Adj SS	Adj MS	F-Value	P-Value
GS, %	10	135.07	13.5069	28.61	0.000
Error	22	10.39	0.4720		
Total	32	145.45			

Model Summary

S	R-sq	R-sq(adj)	R-sq(pred)
0.687057	92.86%	89.61%	83.94%

Comparisons for A22, %

Tukey Pairwise Comparisons: GS, %

Grouping Information Using the Tukey Method and 95% Confidence

GS, %	N	Mean	Grouping				
100.00	3	45.9340	A				
49.69	3	45.4252	A	B			
39.82	3	43.8187		B	C		
29.55	3	42.4288			C	D	
25.42	3	41.9058			C	D	E
20.33	3	40.9300				D	E F
0.00	3	40.8385				D	E F
2.22	3	40.6753				D	E F
14.98	3	40.3533					E F
10.09	3	40.2979					E F
5.05	3	39.8839					F

Means that do not share a letter are significantly different.

General Linear Model: T21, ms versus GS, %

Method

Factor coding (-1; 0; +1)

Factor Information

Factor	Type	Levels	Values
GS, %	Fixed	11	0.00; 2.22; 5.05; 10.09; 14.98; 20.33; 25.42; 29.55; 39.82; 49.69; 100.00

Analysis of Variance

Source	DF	Adj SS	Adj MS	F-Value	P-Value
GS, %	10	8.2863	0.828625	94.32	0.000
Error	22	0.1933	0.008785		
Total	32	8.4795			

Model Summary

S	R-sq	R-sq(adj)	R-sq(pred)
0.0937274	97.72%	96.68%	94.87%

Comparisons for T21, ms

Tukey Pairwise Comparisons: GS, %

Grouping Information Using the Tukey Method and 95% Confidence

GS, %	N	Mean	Grouping
49.69	3	4.09933	A
2.22	3	4.07933	A
5.05	3	4.06500	A
0.00	3	4.01267	A
39.82	3	3.99800	A
29.55	3	3.96533	A
10.09	3	3.95967	A
20.33	3	3.95667	A
25.42	3	3.92833	A
14.98	3	3.92633	A
100.00	3	2.26733	B

Means that do not share a letter are significantly different.

General Linear Model: A21, % versus GS, %

Method

Factor coding (-1; 0; +1)

Factor Information

Factor	Type	Levels	Values
GS, %	Fixed	11	0.00; 2.22; 5.05; 10.09; 14.98; 20.33; 25.42; 29.55; 39.82; 49.69; 100.00

Analysis of Variance

Source	DF	Adj SS	Adj MS	F-Value	P-Value
GS, %	10	135.07	13.5069	28.61	0.000
Error	22	10.39	0.4720		
Total	32	145.45			

Model Summary

S	R-sq	R-sq(adj)	R-sq(pred)
0.687057	92.86%	89.61%	83.94%

Comparisons for A21, %

Tukey Pairwise Comparisons: GS, %

Grouping Information Using the Tukey Method and 95% Confidence

GS, %	N	Mean	Grouping				
5.05	3	60.1161	A				
10.09	3	59.7021	A	B			
14.98	3	59.6467	A	B			
2.22	3	59.3247	A	B	C		
0.00	3	59.1615	A	B	C		
20.33	3	59.0700	A	B	C		
25.42	3	58.0942		B	C	D	
29.55	3	57.5712			C	D	
39.82	3	56.1813				D	E
49.69	3	54.5748					E F
100.00	3	54.0660					F

Means that do not share a letter are significantly different.

General Linear Model: T2, ms versus GS, %

Method

Factor coding (-1; 0; +1)

Factor Information

Factor	Type	Levels	Values
GS, %	Fixed	11	0.00; 2.22; 5.05; 10.09; 14.98; 20.33; 25.42; 29.55; 39.82; 49.69; 100.00

Analysis of Variance

Source	DF	Adj SS	Adj MS	F-Value	P-Value
GS, %	10	3.33554	0.333554	141.51	0.000
Error	22	0.05186	0.002357		
Total	32	3.38739			

Model Summary

S	R-sq	R-sq(adj)	R-sq(pred)
0.0485499	98.47%	97.77%	96.56%

Comparisons for T2, ms

Tukey Pairwise Comparisons: GS, %

Grouping Information Using the Tukey Method and 95% Confidence

GS, %	N	Mean	Grouping
49.69	3	3.10287	A
39.82	3	3.05980	A
5.05	3	3.04333	A
20.33	3	3.04267	A
29.55	3	3.02553	A
14.98	3	3.01870	A
2.22	3	3.00490	A
25.42	3	3.00337	A
10.09	3	3.00000	A
0.00	3	2.96727	A
100.00	3	1.92730	B

Means that do not share a letter are significantly different.

General Linear Model: T1, ms versus GS, %

Method

Factor coding (-1; 0; +1)

Factor Information

Factor	Type	Levels	Values
GS, %	Fixed	11	0.00; 2.22; 5.05; 10.09; 14.98; 20.33; 25.42; 29.55; 39.82; 49.69; 100.00

Analysis of Variance

Source	DF	Adj SS	Adj MS	F-Value	P-Value
GS, %	10	320.684	32.0684	700.18	0.000
Error	22	1.008	0.0458		
Total	32	321.692			

Model Summary

S	R-sq	R-sq(adj)	R-sq(pred)
0.214010	99.69%	99.54%	99.30%

Comparisons for T1, ms

Tukey Pairwise Comparisons: GS, %

Grouping Information Using the Tukey Method and 95% Confidence

GS, %	N	Mean	Grouping					
100.00	3	40.1351	A					
49.69	3	32.9763		B				
39.82	3	31.6769			C			
29.55	3	30.8411				D		
25.42	3	30.3708				D		
20.33	3	30.2261				D	E	
10.09	3	29.6195					E	F
14.98	3	29.5805						F G
5.05	3	28.9772						G H
0.00	3	28.8731						H
2.22	3	28.6335						H

Means that do not share a letter are significantly different.

General Linear Model: MSE Solid Component, % versus GS, %

Method

Factor coding (-1; 0; +1)

Factor Information

Factor	Type	Levels	Values
GS, %	Fixed	11	0.00; 2.22; 5.05; 10.09; 14.98; 20.33; 25.42; 29.55; 39.82; 49.69; 100.00

Analysis of Variance

Source	DF	Adj SS	Adj MS	F-Value	P-Value
GS, %	10	108.159	10.8159	33.75	0.000
Error	22	7.051	0.3205		
Total	32	115.211			

Model Summary

S	R-sq	R-sq(adj)	R-sq(pred)
0.566144	93.88%	91.10%	86.23%

Comparisons for MSE Solid Component, %

Tukey Pairwise Comparisons: GS, %

Grouping Information Using the Tukey Method and 95% Confidence

GS, %	N	Mean	Grouping			
100.00	3	20.0587	A			
49.69	3	16.2103	B			
39.82	3	15.7447	B	C		
29.55	3	15.1777	B	C	D	
25.42	3	14.8533	B	C	D	
20.33	3	14.6590	B	C	D	E
14.98	3	14.2483		C	D	E
10.09	3	14.2140		C	D	E
0.00	3	13.7023			D	E
2.22	3	13.6723			D	E
5.05	3	13.0817				E

Means that do not share a letter are significantly different.

Table 4.5 Pearson Correlation analysis for all factors of GS adulteration determination

Correlation: GS, %; T22, ms; A22, %; T21, ms; A21, %; T2, ms; T1, ms; MSE Solid Component, %; G/W Ratio; Water Activity (aw); Moisture Content, %; Total Soluble Solid, Brix; Glucose, g/100 g; Fructose, g/100 g; Maltose, g/100 g

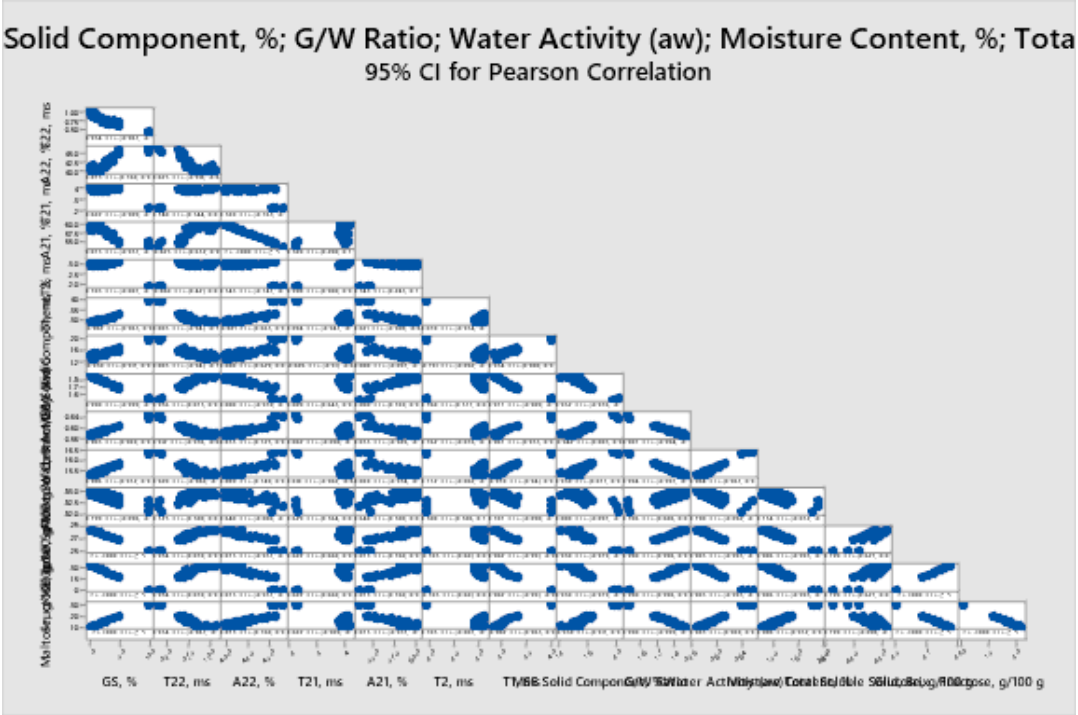

Method

Correlation type	Pearson
Rows used	33

ρ: pairwise Pearson correlation

Correlations

	GS, %	T22, ms	A22, %	T21, ms	A21, %	T2, ms	T1, ms
T22, ms	-0.934						
A22, %	0.875	-0.825					
T21, ms	-0.822	0.748	-0.569				
A21, %	-0.875	0.825	-1.000	0.569			
T2, ms	-0.783	0.668	-0.543	0.990	0.543		
T1, ms	0.982	-0.883	0.821	-0.894	-0.821	-0.870	
MSE Solid Component, %	0.958	-0.883	0.800	-0.826	-0.800	-0.791	0.954
G/W Ratio	-0.998	0.936	-0.880	0.809	0.880	0.768	-0.977
Water Activity (aw)	0.985	-0.912	0.855	-0.802	-0.855	-0.762	0.967
Moisture Content, %	0.986	-0.920	0.869	-0.810	-0.869	-0.772	0.970
Total Soluble Solid, Brix	-0.799	0.725	-0.640	0.629	0.640	0.588	-0.787
Glucose, g/100 g	-1.000	0.934	-0.875	0.822	0.875	0.783	-0.982
Fructose, g/100 g	-1.000	0.934	-0.875	0.822	0.875	0.783	-0.982
Maltose, g/100 g	1.000	-0.934	0.875	-0.822	-0.875	-0.783	0.982

	MSE Solid Component, %	G/W Ratio	Water Activity (aw)	Moisture Content, %	Total Soluble Solid, Brix	Glucose, g/100 g
T22, ms						
A22, %						
T21, ms						
A21, %						
T2, ms						
T1, ms						
MSE Solid Component, %						
G/W Ratio		-0.952				
Water Activity (aw)		0.942	-0.987			
Moisture Content, %		0.938	-0.994	0.984		
Total Soluble Solid, Brix		-0.800	0.786	-0.790	-0.754	
Glucose, g/100 g		-0.958	0.998	-0.985	-0.986	0.799
Fructose, g/100 g		-0.958	0.998	-0.985	-0.986	0.799	1.000
Maltose, g/100 g		0.958	-0.998	0.985	0.986	-0.799	-1.000

	Fructose, g/100 g
T22, ms	
A22, %	
T21, ms	
A21, %	
T2, ms	
T1, ms	
MSE Solid Component, %	
G/W Ratio	
Water Activity (aw)	
Moisture Content, %	
Total Soluble Solid, Brix	
Glucose, g/100 g	
Fructose, g/100 g	
Maltose, g/100 g	-1.000

Pairwise Pearson Correlations

Sample 1	Sample 2	Correlation	95% CI for ρ	P-Value
T22, ms	GS, %	-0.934	(-0.967; -0.870)	0.000
A22, %	GS, %	0.875	(0.760; 0.937)	0.000
T21, ms	GS, %	-0.822	(-0.909; -0.668)	0.000
A21, %	GS, %	-0.875	(-0.937; -0.760)	0.000
T2, ms	GS, %	-0.783	(-0.887; -0.601)	0.000
T1, ms	GS, %	0.982	(0.963; 0.991)	0.000
MSE Solid Component, %	GS, %	0.958	(0.917; 0.979)	0.000
G/W Ratio	GS, %	-0.998	(-0.999; -0.996)	0.000
Water Activity (aw)	GS, %	0.985	(0.969; 0.993)	0.000
Moisture Content, %	GS, %	0.986	(0.972; 0.993)	0.000
Total Soluble Solid, Brix	GS, %	-0.799	(-0.896; -0.627)	0.000
Glucose, g/100 g	GS, %	-1.000	(*; *)	*
Fructose, g/100 g	GS, %	-1.000	(*; *)	*
Maltose, g/100 g	GS, %	1.000	(*; *)	*
A22, %	T22, ms	-0.825	(-0.910; -0.672)	0.000
T21, ms	T22, ms	0.748	(0.544; 0.868)	0.000
A21, %	T22, ms	0.825	(0.672; 0.910)	0.000
T2, ms	T22, ms	0.668	(0.421; 0.823)	0.000
T1, ms	T22, ms	-0.883	(-0.941; -0.775)	0.000
MSE Solid Component, %	T22, ms	-0.883	(-0.941; -0.774)	0.000
G/W Ratio	T22, ms	0.936	(0.873; 0.968)	0.000
Water Activity (aw)	T22, ms	-0.912	(-0.956; -0.829)	0.000
Moisture Content, %	T22, ms	-0.920	(-0.960; -0.842)	0.000
Total Soluble Solid, Brix	T22, ms	0.725	(0.508; 0.855)	0.000
Glucose, g/100 g	T22, ms	0.934	(0.870; 0.967)	0.000
Fructose, g/100 g	T22, ms	0.934	(0.870; 0.967)	0.000
Maltose, g/100 g	T22, ms	-0.934	(-0.967; -0.870)	0.000
T21, ms	A22, %	-0.569	(-0.763; -0.280)	0.001
A21, %	A22, %	-1.000	(*; *)	*
T2, ms	A22, %	-0.543	(-0.747; -0.245)	0.001
T1, ms	A22, %	0.821	(0.665; 0.908)	0.000
MSE Solid Component, %	A22, %	0.800	(0.629; 0.897)	0.000
G/W Ratio	A22, %	-0.880	(-0.939; -0.769)	0.000
Water Activity (aw)	A22, %	0.855	(0.725; 0.926)	0.000
Moisture Content, %	A22, %	0.869	(0.749; 0.934)	0.000
Total Soluble Solid, Brix	A22, %	-0.640	(-0.806; -0.380)	0.000
Glucose, g/100 g	A22, %	-0.875	(-0.937; -0.760)	0.000
Fructose, g/100 g	A22, %	-0.875	(-0.937; -0.760)	0.000
Maltose, g/100 g	A22, %	0.875	(0.760; 0.937)	0.000
A21, %	T21, ms	0.569	(0.280; 0.763)	0.001
T2, ms	T21, ms	0.990	(0.980; 0.995)	0.000
T1, ms	T21, ms	-0.894	(-0.947; -0.794)	0.000
MSE Solid Component, %	T21, ms	-0.826	(-0.911; -0.674)	0.000
G/W Ratio	T21, ms	0.809	(0.645; 0.902)	0.000
Water Activity (aw)	T21, ms	-0.802	(-0.898; -0.632)	0.000
Moisture Content, %	T21, ms	-0.810	(-0.902; -0.646)	0.000
Total Soluble Solid, Brix	T21, ms	0.629	(0.364; 0.800)	0.000
Glucose, g/100 g	T21, ms	0.822	(0.668; 0.909)	0.000
Fructose, g/100 g	T21, ms	0.822	(0.668; 0.909)	0.000
Maltose, g/100 g	T21, ms	-0.822	(-0.909; -0.668)	0.000
T2, ms	A21, %	0.543	(0.245; 0.747)	0.001
T1, ms	A21, %	-0.821	(-0.908; -0.665)	0.000
MSE Solid Component, %	A21, %	-0.800	(-0.897; -0.629)	0.000

G/W Ratio	A21, %	0.880	(0.769; 0.939)	0.000
Water Activity (aw)	A21, %	-0.855	(-0.926; -0.725)	0.000
Moisture Content, %	A21, %	-0.869	(-0.934; -0.749)	0.000
Total Soluble Solid, Brix	A21, %	0.640	(0.380; 0.806)	0.000
Glucose, g/100 g	A21, %	0.875	(0.760; 0.937)	0.000
Fructose, g/100 g	A21, %	0.875	(0.760; 0.937)	0.000
Maltose, g/100 g	A21, %	-0.875	(-0.937; -0.760)	0.000
T1, ms	T2, ms	-0.870	(-0.934; -0.751)	0.000
MSE Solid Component, %	T2, ms	-0.791	(-0.892; -0.615)	0.000
G/W Ratio	T2, ms	0.768	(0.577; 0.880)	0.000
Water Activity (aw)	T2, ms	-0.762	(-0.876; -0.567)	0.000
Moisture Content, %	T2, ms	-0.772	(-0.882; -0.584)	0.000
Total Soluble Solid, Brix	T2, ms	0.588	(0.306; 0.775)	0.000
Glucose, g/100 g	T2, ms	0.783	(0.601; 0.887)	0.000
Fructose, g/100 g	T2, ms	0.783	(0.601; 0.887)	0.000
Maltose, g/100 g	T2, ms	-0.783	(-0.887; -0.601)	0.000
MSE Solid Component, %	T1, ms	0.954	(0.908; 0.977)	0.000
G/W Ratio	T1, ms	-0.977	(-0.989; -0.953)	0.000
Water Activity (aw)	T1, ms	0.967	(0.933; 0.984)	0.000
Moisture Content, %	T1, ms	0.970	(0.941; 0.985)	0.000
Total Soluble Solid, Brix	T1, ms	-0.787	(-0.890; -0.608)	0.000
Glucose, g/100 g	T1, ms	-0.982	(-0.991; -0.963)	0.000
Fructose, g/100 g	T1, ms	-0.982	(-0.991; -0.963)	0.000
Maltose, g/100 g	T1, ms	0.982	(0.963; 0.991)	0.000
G/W Ratio	MSE Solid Component, %	-0.952	(-0.976; -0.904)	0.000
Water Activity (aw)	MSE Solid Component, %	0.942	(0.885; 0.971)	0.000
Moisture Content, %	MSE Solid Component, %	0.938	(0.877; 0.969)	0.000
Total Soluble Solid, Brix	MSE Solid Component, %	-0.800	(-0.897; -0.630)	0.000
Glucose, g/100 g	MSE Solid Component, %	-0.958	(-0.979; -0.917)	0.000
Fructose, g/100 g	MSE Solid Component, %	-0.958	(-0.979; -0.917)	0.000
Maltose, g/100 g	MSE Solid Component, %	0.958	(0.917; 0.979)	0.000
Water Activity (aw)	G/W Ratio	-0.987	(-0.994; -0.974)	0.000
Moisture Content, %	G/W Ratio	-0.994	(-0.997; -0.988)	0.000
Total Soluble Solid, Brix	G/W Ratio	0.786	(0.606; 0.889)	0.000
Glucose, g/100 g	G/W Ratio	0.998	(0.996; 0.999)	0.000
Fructose, g/100 g	G/W Ratio	0.998	(0.996; 0.999)	0.000
Maltose, g/100 g	G/W Ratio	-0.998	(-0.999; -0.996)	0.000
Moisture Content, %	Water Activity (aw)	0.984	(0.967; 0.992)	0.000
Total Soluble Solid, Brix	Water Activity (aw)	-0.790	(-0.892; -0.614)	0.000
Glucose, g/100 g	Water Activity (aw)	-0.985	(-0.993; -0.969)	0.000
Fructose, g/100 g	Water Activity (aw)	-0.985	(-0.993; -0.969)	0.000
Maltose, g/100 g	Water Activity (aw)	0.985	(0.969; 0.993)	0.000
Total Soluble Solid, Brix	Moisture Content, %	-0.754	(-0.872; -0.554)	0.000
Glucose, g/100 g	Moisture Content, %	-0.986	(-0.993; -0.972)	0.000
Fructose, g/100 g	Moisture Content, %	-0.986	(-0.993; -0.972)	0.000
Maltose, g/100 g	Moisture Content, %	0.986	(0.972; 0.993)	0.000
Glucose, g/100 g	Total Soluble Solid, Brix	0.799	(0.627; 0.896)	0.000
Fructose, g/100 g	Total Soluble Solid, Brix	0.799	(0.627; 0.896)	0.000
Maltose, g/100 g	Total Soluble Solid, Brix	-0.799	(-0.896; -0.627)	0.000
Fructose, g/100 g	Glucose, g/100 g	1.000	(*; *)	*
Maltose, g/100 g	Glucose, g/100 g	-1.000	(*; *)	*
Maltose, g/100 g	Fructose, g/100 g	-1.000	(*; *)	*

C. Extra Figures

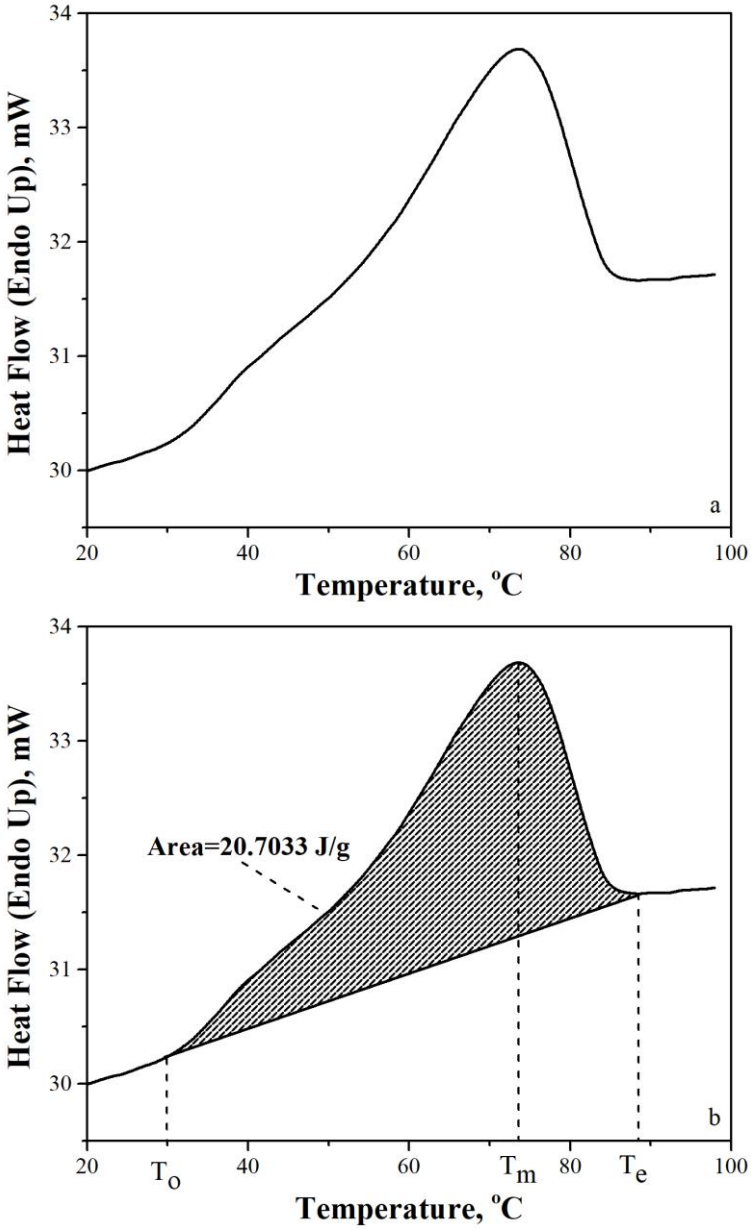

Figure 4.1. Representative thermogram for heating of crystallized honey sample (36^{th} hour) (a) and calculation of process temperatures and area under curve (b) where T_o, T_m and T_e denote onset, melting and end set temperature values, respectively